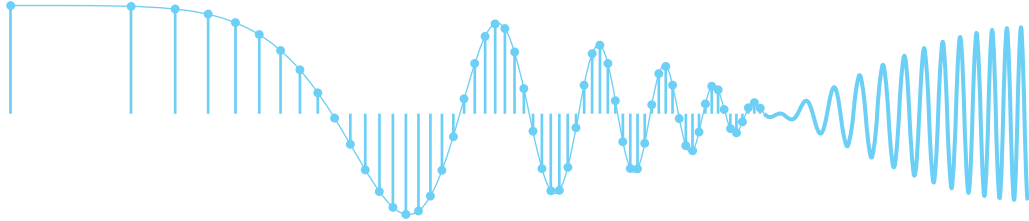


C H A P T E R 7



Discrete-Time Fourier Transform

In Chapter 3 and Appendix C, we showed that interesting continuous-time waveforms $x(t)$ can be synthesized by summing sinusoids, or complex exponential signals, having different frequencies f_k and complex amplitudes a_k . We also introduced the concept of the *spectrum* of a signal as the collection of information about the frequencies and corresponding complex amplitudes $\{f_k, a_k\}$ of the complex exponential signals, and found it convenient to display the spectrum as a plot of spectrum lines versus frequency, each labeled with amplitude and phase. This spectrum plot is a *frequency-domain representation* that tells us at a glance “how much of each frequency is present in the signal.”

In Chapter 4, we extended the spectrum concept from continuous-time signals $x(t)$ to discrete-time signals $x[n]$ obtained by sampling $x(t)$. In the discrete-time case, the line spectrum is plotted as a function of normalized frequency $\hat{\omega}$. In Chapter 6, we developed the frequency response $H(e^{j\hat{\omega}})$ which is the frequency-domain representation of an FIR filter. Since an FIR filter can also be characterized in the time domain by its impulse response signal $h[n]$, it is not hard to imagine that the frequency response is the *frequency-domain representation*, or *spectrum*, of the sequence $h[n]$.

In this chapter, we take the next step by developing the *discrete-time Fourier transform (DTFT)*. The DTFT is a frequency-domain representation for a wide range of both finite- and infinite-length discrete-time signals $x[n]$. The DTFT is denoted as $X(e^{j\hat{\omega}})$, which shows that the frequency dependence always includes the complex exponential function $e^{j\hat{\omega}}$. The operation of taking the Fourier transform of a signal will become a common tool for analyzing signals and systems *in the frequency domain*.¹

The application of the DTFT is usually called Fourier analysis, or spectrum analysis or “going into the Fourier domain or frequency domain.” Thus, the words spectrum, Fourier, and frequency-domain representation become equivalent, even though each one retains its own distinct character.

7-1 DTFT: Fourier Transform for Discrete-Time Signals

The concept of frequency response discussed in Chapter 6 emerged from analysis showing that if an input to an LTI discrete-time system is of the form $x[n] = e^{j\hat{\omega}n}$, then the corresponding output has the form $y[n] = H(e^{j\hat{\omega}})e^{j\hat{\omega}n}$, where $H(e^{j\hat{\omega}})$ is called the frequency response of the LTI system. This fact, coupled with the principle of superposition for LTI systems leads to the fundamental result that the frequency response function $H(e^{j\hat{\omega}})$ is sufficient to determine the output due to any linear combination of signals of the form $e^{j\hat{\omega}n}$ or $\cos(\hat{\omega}n + \theta)$. For discrete-time filters such as the causal FIR filters discussed in Chapter 6, the frequency response function is obtained from the summation formula

$$H(e^{j\hat{\omega}}) = \sum_{n=0}^M h[n]e^{-j\hat{\omega}n} = h[0] + h[1]e^{-j\hat{\omega}} + \dots + h[M]e^{-j\hat{\omega}M} \quad (7.1)$$

where $h[n]$ is the impulse response. In a mathematical sense, the impulse response $h[n]$ is *transformed* into the frequency response by the operation of evaluating (7.1) for each value of $\hat{\omega}$ over the domain $-\pi < \hat{\omega} \leq \pi$. The operation of transformation (adding up the terms in (7.1) for each value $\hat{\omega}$) replaces a function of a discrete-time index n (a sequence) by a periodic function of the continuous frequency variable $\hat{\omega}$. By this transformation, the time-domain representation $h[n]$ is replaced by the frequency-domain representation $H(e^{j\hat{\omega}})$. For this notion to be complete and useful, we need to know that the result of the transformation is unique, and we need the ability to go back from the frequency-domain representation to the time-domain representation. That is, we need an *inverse transform* that recovers the original $h[n]$ from $H(e^{j\hat{\omega}})$. In Chapter 6, we showed that the sequence can be reconstructed from a frequency response represented in terms of powers of $e^{-j\hat{\omega}}$ as in (7.1) by simply picking off the coefficients of the polynomial since, $h[n]$ is the coefficient of $e^{-j\hat{\omega}n}$. While this process can be effective if M is small, there is a much more powerful approach to inverting the transformation that holds even for infinite-length sequences.

¹It is common in engineering to say that we “take the discrete-time Fourier transform” when we mean that we consider $X(e^{j\hat{\omega}})$ as our representation of a signal $x[n]$.

In this section, we show that the frequency response is identical to the result of applying the more general concept of the DTFT to the impulse response of the LTI system. We give an integral form for the inverse DTFT that can be used even when $H(e^{j\hat{\omega}})$ does not have a finite polynomial representation such as (7.1). Furthermore, we show that the DTFT can be used to represent a wide range of sequences, including sequences of infinite length, and that these sequences can be impulse responses, inputs to LTI systems, outputs of LTI systems, or indeed, any sequence that satisfies certain conditions to be discussed in this chapter.

7-1.1 Forward DTFT

The DTFT of a sequence $x[n]$ is defined as

Discrete-Time Fourier Transform

$$X(e^{j\hat{\omega}}) = \sum_{n=-\infty}^{\infty} x[n]e^{-j\hat{\omega}n} \quad (7.2)$$

The DTFT $X(e^{j\hat{\omega}})$ that results from the definition is a function of frequency $\hat{\omega}$. Going from the signal $x[n]$ to its DTFT is referred to as “taking the forward transform,” and going from the DTFT back to the signal is referred to as “taking the inverse transform.” The limits on the sum in (7.2) are shown as infinite so that the DTFT defined for infinitely long signals as well as finite-length signals.² However, a comparison of (7.2) to (7.1) shows that if the sequence were a finite-length impulse response, then the DTFT of that sequence would be the same as the frequency response of the FIR system. More generally, if $h[n]$ is the impulse response of an LTI system, then the DTFT of $h[n]$ is the frequency response $H(e^{j\hat{\omega}})$ of that system. Examples of infinite-duration impulse response filters will be given in Chapter 10.

EXERCISE 7.1

Show that the DTFT function $X(e^{j\hat{\omega}})$ defined in (7.2) is always periodic in $\hat{\omega}$ with period 2π , that is,

$$X(e^{j(\hat{\omega}+2\pi)}) = X(e^{j\hat{\omega}}).$$

7-1.2 DTFT of a Shifted Impulse Sequence

Our first task is to develop examples of the DTFT for some common signals. The simplest case is the time-shifted unit-impulse sequence $x[n] = \delta[n - n_0]$. Its forward DTFT is by definition

$$X(e^{j\hat{\omega}}) = \sum_{n=-\infty}^{\infty} \delta[n - n_0]e^{-j\hat{\omega}n}$$

²The infinite limits are used to imply that the sum is over all n , where $x[n] \neq 0$. This often avoids unnecessarily awkward expressions when using the DTFT for analysis.

Since the impulse sequence is nonzero only at $n = n_0$ it follows that the sum has only one nonzero term, so

$$X(e^{j\hat{\omega}}) = e^{-j\hat{\omega}n_0}$$

To emphasize the importance of this and other DTFT relationships, we use the notation $\overset{\text{DTFT}}{\longleftrightarrow}$ to denote the forward and inverse transforms in one statement:

$$\boxed{\begin{array}{l} \text{DTFT Representation of } \delta[n - n_0] \\ x[n] = \delta[n - n_0] \overset{\text{DTFT}}{\longleftrightarrow} X(e^{j\hat{\omega}}) = e^{-j\hat{\omega}n_0} \end{array}} \quad (7.3)$$

7-1.3 Linearity of the DTFT

Before we proceed further in our discussion of the DTFT, it is useful to consider one of its most important properties. The DTFT is a linear operation; that is, the DTFT of a sum of two or more scaled signals results in the identical sum and scaling of their corresponding DTFTs. To verify this, assume that $x[n] = ax_1[n] + bx_2[n]$, where a and b are (possibly complex) constants. The DTFT of $x[n]$ is by definition

$$X(e^{j\hat{\omega}}) = \sum_{n=-\infty}^{\infty} (ax_1[n] + bx_2[n])e^{-j\hat{\omega}n}$$

If both $x_1[n]$ and $x_2[n]$ have DTFTs, then we can use the algebraic property that multiplication distributes over addition to write

$$X(e^{j\hat{\omega}}) = a \sum_{n=-\infty}^{\infty} x_1[n]e^{-j\hat{\omega}n} + b \sum_{n=-\infty}^{\infty} x_2[n]e^{-j\hat{\omega}n} = aX_1(e^{j\hat{\omega}}) + bX_2(e^{j\hat{\omega}})$$

That is, the frequency-domain representations are combined in exactly the same way as the signals are combined.

EXAMPLE 7-1 DTFT of an FIR Filter

The following FIR filter

$$y[n] = 5x[n - 1] - 4x[n - 3] + 3x[n - 5]$$

has a finite-length impulse response signal:

$$h[n] = 5\delta[n - 1] - 4\delta[n - 3] + 3\delta[n - 5]$$

Each impulse in $h[n]$ is transformed using (7.3), and then combined according to the linearity property of the DTFT which gives

$$H(e^{j\hat{\omega}}) = 5e^{-j\hat{\omega}} - 4e^{-j3\hat{\omega}} + 3e^{-j5\hat{\omega}}$$

7-1.4 Uniqueness of the DTFT

The DTFT is a *unique* relationship between $x[n]$ and $X(e^{j\hat{\omega}})$; in other words, two different signals cannot have the same DTFT. This is a consequence of the linearity property because if two different signals have the same DTFT, then we can form a third signal by subtraction and obtain

$$x_3[n] = x_1[n] - x_2[n] \xleftrightarrow{\text{DTFT}} X_3(e^{j\hat{\omega}}) = \underbrace{X_1(e^{j\hat{\omega}}) - X_2(e^{j\hat{\omega}})}_{\text{identical DTFTs}} = 0$$

However, from the definition (7.2) it is easy to argue that $x_3[n]$ has to be zero if its DTFT is zero, which in turn implies that $x_1[n] = x_2[n]$.

The importance of uniqueness is that if we know a DTFT representation such as (7.3), we can start in either the time or frequency domain and easily write down the corresponding representation in the other domain. For example, if $X(e^{j\hat{\omega}}) = e^{-j\hat{\omega}3}$ then we know that $x[n] = \delta[n - 3]$.

7-1.5 DTFT of a Pulse

Another common signal is the L -point rectangular pulse, which is a finite-length time signal consisting of all ones:

$$r_L[n] = u[n] - u[n - L] = \begin{cases} 1 & n = 0, 1, 2, \dots, L - 1 \\ 0 & \text{elsewhere} \end{cases}$$

Its forward DTFT is by definition

$$R_L(e^{j\hat{\omega}}) = \sum_{n=0}^{L-1} 1 e^{-j\hat{\omega}n} = \frac{1 - e^{-j\hat{\omega}L}}{1 - e^{-j\hat{\omega}}} \quad (7.4)$$

where we have used the formula for the sum of L terms of a geometric series to “sum” the series and obtain a closed-form expression for $R_L(e^{j\hat{\omega}})$. This is a signal that we studied before in Chapter 6 as the impulse response of an L -point running-sum filter. In Section 6-7, the frequency response of the running-sum filter was shown to be the product of a Dirichlet form and a complex exponential. Referring to the earlier results in Section 6-7 or further manipulating (7.4), we obtain another DTFT pair:

DTFT Representation of L -Point Rectangular Pulse

$$r_L[n] = u[n] - u[n - L] \xleftrightarrow{\text{DTFT}} R_L(e^{j\hat{\omega}}) = \frac{\sin(L\hat{\omega}/2)}{\sin(\hat{\omega}/2)} e^{-j\hat{\omega}(L-1)/2} \quad (7.5)$$

Since the filter coefficients of the running-sum filter are L times the filter coefficients of the running-average filter, there is no L in the denominator of (7.5).

7-1.6 DTFT of a Right-Sided Exponential Sequence

As an illustration of the DTFT of an infinite-duration sequence, consider a “right-sided” exponential signal of the form $x[n] = a^n u[n]$, where a can be real or complex. Such a signal is zero for $n < 0$ (on the *left-hand side* of a plot). It decays “exponentially” for $n \geq 0$ if $|a| < 1$; it remains constant at 1 if $|a| = 1$; and it grows exponentially if $|a| > 1$. Its DTFT is by definition

$$X(e^{j\hat{\omega}}) = \sum_{n=-\infty}^{\infty} a^n u[n] e^{-j\hat{\omega}n} = \sum_{n=0}^{\infty} a^n e^{-j\hat{\omega}n}$$

We can obtain a closed-form expression for $X(e^{j\hat{\omega}})$ by noting that

$$X(e^{j\hat{\omega}}) = \sum_{n=0}^{\infty} (ae^{-j\hat{\omega}})^n$$

which can now be recognized as the sum of all the terms of an infinite geometric series, where the ratio between successive terms is $(ae^{-j\hat{\omega}})$. For such a series there is a formula for the sum that we can apply to give the final result

$$X(e^{j\hat{\omega}}) = \sum_{n=0}^{\infty} (ae^{-j\hat{\omega}})^n = \frac{1}{1 - ae^{-j\hat{\omega}}}$$

There is one limitation, however. Going from the infinite sum to the closed-form result is only valid when $|ae^{-j\hat{\omega}}| < 1$ or $|a| < 1$. Otherwise, the terms in the geometric series grow without bound and their sum is infinite.

This DTFT pair is another widely used result, worthy of highlighting as we have done with the shifted impulse and pulse sequences.

| |
|---|
| <p style="color: #00AEEF; margin: 0;">DTFT Representation of $a^n u[n]$</p> $x[n] = a^n u[n] \xleftrightarrow{\text{DTFT}} X(e^{j\hat{\omega}}) = \frac{1}{1 - ae^{-j\hat{\omega}}} \quad \text{if } a < 1 \tag{7.6}$ |
|---|

EXERCISE 7.2

Use the uniqueness property of the DTFT along with (7.6) to find $x[n]$ whose DTFT is

$$X(e^{j\hat{\omega}}) = \frac{1}{1 - 0.5e^{-j\hat{\omega}}}$$

EXERCISE 7.3

Use the linearity of the DTFT and (7.6) to determine the DTFT of the following sum of two right-sided exponential signals: $x[n] = (0.8)^n u[n] + 2(-0.5)^n u[n]$.

7-1.7 Existence of the DTFT

In the case of finite-length sequences such as the impulse response of an FIR filter, the sum defining the DTFT has a finite number of terms. Thus, the DTFT of an FIR filter as in (7.1) always exists because $X(e^{j\hat{\omega}})$ is always finite. However, in the general case, where one or both of the limits on the sum in (7.2) are infinite, the DTFT sum may diverge (become infinite). This is illustrated by the right-sided exponential sequence in Section 7-1.6 when $|a| > 1$.

A sufficient condition for the existence of the DTFT of a sequence $x[n]$ emerges from the following manipulation that develops a bound on the size of $X(e^{j\hat{\omega}})$:

$$\begin{aligned}
 |X(e^{j\hat{\omega}})| &= \left| \sum_{n=-\infty}^{\infty} x[n]e^{-j\hat{\omega}n} \right| \\
 &\leq \sum_{n=-\infty}^{\infty} |x[n]e^{-j\hat{\omega}n}| \quad (\text{magnitude of sum} \leq \text{sum of magnitudes}) \\
 &= \sum_{n=-\infty}^{\infty} |x[n]| \underbrace{|e^{-j\hat{\omega}n}|}_{\nearrow 1} \quad (\text{magnitude of product} = \text{product of magnitudes}) \\
 &= \sum_{n=-\infty}^{\infty} |x[n]|
 \end{aligned}$$

It follows that a sufficient condition for the existence of the DTFT of $x[n]$ is

Sufficient Condition for Existence of the DTFT

$$|X(e^{j\hat{\omega}})| \leq \sum_{n=-\infty}^{\infty} |x[n]| < \infty \quad (7.7)$$

A sequence $x[n]$ satisfying (7.7) is said to be *absolutely summable*, and when (7.7) holds, the infinite sum defining the DTFT $X(e^{j\hat{\omega}})$ in (7.2) is said to *converge* to a finite result for all $\hat{\omega}$.

EXAMPLE 7-2 DTFT of Complex Exponential?

Consider a right-sided complex exponential sequence, $x[n] = re^{j\hat{\omega}_0 n} u[n]$ when $r = 1$. Applying the condition of (7.7) to this sequence leads to

$$\sum_{n=0}^{\infty} |e^{j\hat{\omega}_0 n}| = \sum_{n=0}^{\infty} 1 \rightarrow \infty$$

Thus, the DTFT of a right-sided complex exponential is not guaranteed to exist, and it is easy to verify that $|X(e^{j\hat{\omega}_0})| \rightarrow \infty$. On the other hand, if $r < 1$, the DTFT of $x[n] = r^n e^{j\hat{\omega}_0 n} u[n]$ exists and is given by the result of Section 7-1.6 with $a = re^{j\hat{\omega}_0}$. The non-existence of the DTFT is also true for the related case of a two-sided sinusoid, defined as $e^{j\hat{\omega}_0 n}$ for $-\infty < n < \infty$.

7-1.8 The Inverse DTFT

Now that we have a condition for the existence of the DTFT, we need to address the question of the inverse DTFT. The uniqueness property implies that if we have a table of known DTFT pairs such as (7.3), (7.5), and (7.6), we can always go back and forth between the time-domain and frequency-domain representations simply by table lookup as in Exercise 7.2. However, with this approach, we would always be limited by the size of our table of known DTFT pairs.

Instead, we want to continue the development of the DTFT by studying a general expression for performing the inverse DTFT. The DTFT $X(e^{j\hat{\omega}})$ is a function of the continuous variable $\hat{\omega}$, so an integral (7.8) with respect to normalized frequency $\hat{\omega}$ is needed to transform $X(e^{j\hat{\omega}})$ back to the sequence $x[n]$.

$$\boxed{\begin{array}{c} \textit{Inverse DTFT} \\ x[n] = \frac{1}{2\pi} \int_{-\pi}^{\pi} X(e^{j\hat{\omega}}) e^{j\hat{\omega}n} d\hat{\omega}. \end{array}} \quad (7.8)$$

Observe that n is an integer parameter in the integral, while $\hat{\omega}$ now is a dummy variable of integration that disappears when the definite integral is evaluated at its limits. The variable n can take on all integer values in the range $-\infty < n < \infty$, and hence, using (7.8) we can extract each sample of a sequence $x[n]$ whose DTFT is $X(e^{j\hat{\omega}})$. We could verify that (7.8) is the correct inverse DTFT relation by substituting the definition of the DTFT in (7.2) into (7.8) and rearranging terms.

Instead of carrying out a general proof, we present a simpler and more intuitive justification by working with the shifted impulse sequence $\delta[n - n_0]$, whose DTFT is known to be

$$X(e^{j\hat{\omega}}) = e^{-j\hat{\omega}n_0}$$

The objective is to show that (7.8) gives the correct time-domain result when operating on $X(e^{j\hat{\omega}})$. If we substitute this DTFT into (7.8), we obtain

$$\frac{1}{2\pi} \int_{-\pi}^{\pi} X(e^{j\hat{\omega}}) e^{j\hat{\omega}n} d\hat{\omega} = \frac{1}{2\pi} \int_{-\pi}^{\pi} e^{-j\hat{\omega}n_0} e^{j\hat{\omega}n} d\hat{\omega} = \frac{1}{2\pi} \int_{-\pi}^{\pi} e^{j\hat{\omega}(n-n_0)} d\hat{\omega} \quad (7.9)$$

The definite integral of the exponential must be treated as two cases: first, when $n = n_0$,

$$\frac{1}{2\pi} \int_{-\pi}^{\pi} e^{j\hat{\omega}(n-n_0)} d\hat{\omega} = \frac{1}{2\pi} \int_{-\pi}^{\pi} d\hat{\omega} = 1 \quad (7.10a)$$

and then for $n \neq n_0$,

$$\frac{1}{2\pi} \int_{-\pi}^{\pi} e^{j\hat{\omega}(n-n_0)} d\hat{\omega} = \frac{1}{2\pi} \left. \frac{e^{j\hat{\omega}(n-n_0)}}{j(n-n_0)} \right|_{-\pi}^{\pi} = \frac{e^{j\pi(n-n_0)} - e^{-j\pi(n-n_0)}}{j2\pi(n-n_0)} = 0 \quad (7.10b)$$

Equations (7.10a) and (7.10b) show that the complex exponentials $e^{j\hat{\omega}n}$ and $e^{-j\hat{\omega}n_0}$ (when viewed as periodic functions of $\hat{\omega}$) are *orthogonal* to each other.³

Putting these two cases together, we have

$$\frac{1}{2\pi} \int_{-\pi}^{\pi} e^{-j\hat{\omega}n_0} e^{j\hat{\omega}n} d\hat{\omega} = \begin{cases} 1 & n = n_0 \\ 0 & n \neq n_0 \end{cases} = \delta[n - n_0] \quad (7.11)$$

Thus, we have shown that (7.8) correctly returns the sequence $x[n] = \delta[n - n_0]$, when the DTFT is $X(e^{j\hat{\omega}}) = e^{-j\hat{\omega}n_0}$.

This example is actually strong enough to justify that the inverse DTFT integral (7.8) will always work, because the DTFT of a general finite-length sequence is always a linear combination of complex exponential terms like $e^{-j\hat{\omega}n_0}$. The linearity property of the DTFT, therefore, guarantees that the inverse DTFT integral will recover a finite-length sequence that is the same linear combination of shifted impulses, which is the correct sequence for a finite-length signal. If the signal is of infinite extent, it can be shown that if $x[n]$ is absolutely summable as in (7.7) so that the DTFT exists, then (7.8) recovers the original sequence from $X(e^{j\hat{\omega}})$.

EXERCISE 7.4

Recall that $X(e^{j\hat{\omega}})$ defined in (7.2) is always periodic in $\hat{\omega}$ with period 2π . Use this fact and a change of variables to argue that we can rewrite the inverse DTFT integral with limits that go from 0 to 2π , instead of $-\pi$ to $+\pi$; that is, show that

$$\frac{1}{2\pi} \int_{-\pi}^{\pi} X(e^{j\hat{\omega}}) e^{j\hat{\omega}n} d\hat{\omega} = \frac{1}{2\pi} \int_0^{2\pi} X(e^{j\hat{\omega}}) e^{j\hat{\omega}n} d\hat{\omega}$$

7-1.9 Bandlimited DTFT

Ordinarily we define a signal in the time domain, but the inverse DTFT integral enables us to define a signal in the frequency domain by specifying its DTFT as a function of frequency. Once we specify the magnitude and phase of $X(e^{j\hat{\omega}})$, we apply (7.8) and carry out the integral to get the signal $x[n]$. An excellent example of this process is to define an *ideal bandlimited signal*, which is a function that is nonzero in the low frequency band $|\hat{\omega}| \leq \hat{\omega}_b$ and zero in the high frequency band $\hat{\omega}_b < \hat{\omega} \leq \pi$. If the nonzero portion of the DTFT is a constant value of one with a phase of zero, then we have

$$X(e^{j\hat{\omega}}) = \begin{cases} 1 & |\hat{\omega}| \leq \hat{\omega}_b \\ 0 & \hat{\omega}_b < |\hat{\omega}| \leq \pi \end{cases}$$

which is plotted in Fig. 7-1(a).

³This same property was used in Section 3-5 to derive the Fourier series integral for periodic continuous-time signals. Note for example, the similarity between equations (3.27) and (7.8).

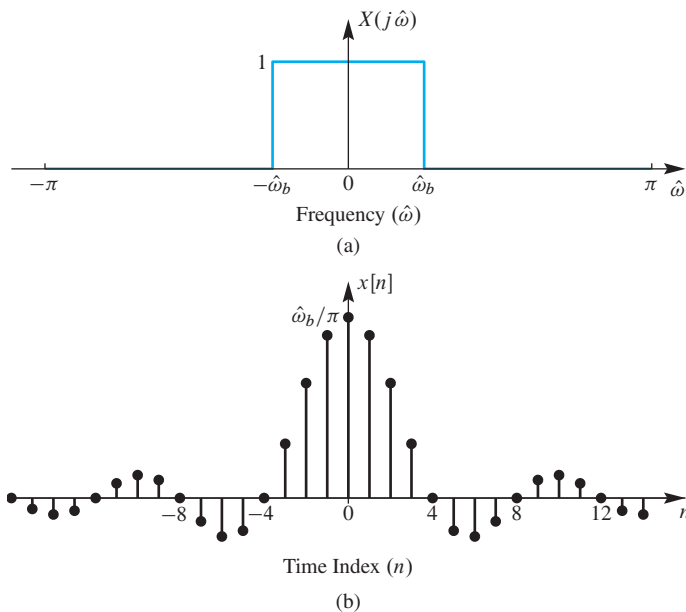


Figure 7-1 Bandlimited DTFT. (a) DTFT is a rectangle bandlimited to $\hat{\omega}_b = 0.25\pi$. (b) Inverse DTFT is a sampled sinc function.

For this simple DTFT function, the integrand of (7.8) has a piecewise constant function that is relatively easy to integrate after we substitute the definition of $X(e^{j\hat{\omega}})$ into the inverse DTFT integral (7.8)

$$\begin{aligned}
 x[n] &= \frac{1}{2\pi} \int_{-\pi}^{\pi} X(e^{j\hat{\omega}}) e^{j\hat{\omega}n} d\hat{\omega} = \frac{1}{2\pi} \int_{-\pi}^{-\hat{\omega}_b} 0 e^{j\hat{\omega}n} d\hat{\omega} \\
 &\quad + \frac{1}{2\pi} \int_{-\hat{\omega}_b}^{\hat{\omega}_b} 1 e^{j\hat{\omega}n} d\hat{\omega} + \frac{1}{2\pi} \int_{\hat{\omega}_b}^{\pi} 0 e^{j\hat{\omega}n} d\hat{\omega}
 \end{aligned}$$

The integral has been broken into three cases for the three intervals, where $X(e^{j\hat{\omega}})$ is either zero or one. Only the middle integral is nonzero, and the integration yields

$$\begin{aligned}
 x[n] &= \frac{1}{2\pi} \int_{-\hat{\omega}_b}^{\hat{\omega}_b} 1 e^{j\hat{\omega}n} d\hat{\omega} \\
 &= \frac{e^{j\hat{\omega}n}}{2\pi jn} \Big|_{-\hat{\omega}_b}^{\hat{\omega}_b} = \frac{e^{j\hat{\omega}_b n} - e^{-j\hat{\omega}_b n}}{(2j)\pi n} = \frac{\sin(\hat{\omega}_b n)}{\pi n}
 \end{aligned}$$

The last step uses the inverse Euler's formula for sine.

The result of the inverse DTFT is the discrete-time signal

$$x[n] = \frac{\sin(\hat{\omega}_b n)}{\pi n} \quad -\infty < n < \infty \quad (7.12)$$

where $0 < \hat{\omega}_b < \pi$. This mathematical form, which is called a “sinc function,” is plotted in Fig. 7-1(b) for $\hat{\omega}_b = 0.25\pi$. Although the “sinc function” appears to be undefined at $n = 0$, a careful application of L’Hôpital’s rule, or the small angle approximation to the sine function, shows that the value is actually $x[0] = \hat{\omega}_b/\pi$. Since a DTFT pair is unique, we have obtained another DTFT pair that can be added to our growing inventory.

DTFT Representation of a Sinc Function

$$x[n] = \frac{\sin(\hat{\omega}_b n)}{\pi n} \stackrel{\text{DTFT}}{\longleftrightarrow} X(e^{j\hat{\omega}}) = \begin{cases} 1 & |\hat{\omega}| \leq \hat{\omega}_b \\ 0 & \text{otherwise} \end{cases} \quad (7.13)$$

We will revisit this transform as a frequency response in Section 7-3 when discussing ideal filters.

Our usage of the term “sinc function” refers to a form, rather than a specific function definition. The form of the “sinc function” has a sine function in the numerator and the variable in the denominator. In signal processing, the normalized sinc function is defined as

$$\text{sinc}(\theta) = \frac{\sin \pi \theta}{\pi \theta}$$

and this is the definition used in the MATLAB M-file `sinc`. If we expressed $x[n]$ in (7.12) in terms of this definition of the sinc function, we would write

$$x[n] = \frac{\hat{\omega}_b}{\pi} \text{sinc}\left(\frac{\hat{\omega}_b}{\pi} n\right)$$

While it is nice to have the name sinc for this function, which turns up often in Fourier transform expressions, it can be cumbersome to figure out the proper argument and scaling. On the other hand, the term “sinc function” is widely used as a convenient shorthand for any function of the general form of (7.12), so we use the term henceforth in that sense.

The sinc signal is important in discrete-time signal and system theory, but it is impossible to determine its DTFT by directly applying the forward transform summation (7.2). This can be seen by writing out the forward DTFT of a sinc function, which is the infinite summation on the left-hand side below.

$$X(e^{j\hat{\omega}}) = \sum_{n=-\infty}^{\infty} \frac{\sin(\hat{\omega}_b n)}{\pi n} e^{-j\hat{\omega} n} = \begin{cases} 1 & |\hat{\omega}| \leq \hat{\omega}_b \\ 0 & \text{otherwise} \end{cases} \quad (7.14)$$

However, because of the uniqueness of the DTFT, we have obtained the desired DTFT transform pair by starting in the frequency domain with the correct transform $X(e^{j\hat{\omega}})$ and taking the inverse DTFT of $X(e^{j\hat{\omega}})$ to get the “sinc function” sequence.

Another property of the sinc function sequence is that it is not absolutely summable. If we recall from (7.7) that absolute summability is a *sufficient condition* for the DTFT to exist, then the sinc function must be an exception. We know that its DTFT exists because the right-hand side of (7.14) is finite and well defined. Therefore, the transform pair (7.13) shows that the condition of absolute summability is a sufficient, but not a necessary condition, for the existence of the DTFT.

7-1.10 Inverse DTFT for the Right-Sided Exponential

Another infinite-length sequence is the right-sided exponential signal $x[n] = a^n u[n]$ discussed in Section 7-1.6. In this case, we were able to use a familiar result for geometric series to “sum” the expression for the DTFT and obtain a closed-form representation

$$X(e^{j\hat{\omega}}) = \frac{1}{1 - ae^{-j\hat{\omega}}} \quad |a| < 1 \quad (7.15)$$

On the other hand, suppose that we want to determine $x[n]$ given $X(e^{j\hat{\omega}})$ in (7.15). Substituting this into the inverse DTFT expression (7.8) gives

$$x[n] = \frac{1}{2\pi} \int_{-\pi}^{\pi} \frac{e^{j\hat{\omega}n}}{1 - ae^{-j\hat{\omega}}} d\hat{\omega} \quad (7.16)$$

Although techniques exist for evaluating such integrals using the theory of complex variables, we do not assume knowledge of these techniques. However, all is not lost, because the uniqueness property of the DTFT tells us that we can always rely on the tabulated result in (7.6), and we can write the inverse transform by inspection. The important point of this example and the sinc function example is that once a transform pair has been determined, by whatever means, we can use that DTFT relationship to move back and forth between the time and frequency domains without integrals or sums. Furthermore, in Section 7-2 we will introduce a number of general properties of the DTFT that can be employed to simplify forward and inverse DTFT manipulations even more.

7-1.11 The DTFT Spectrum

So far, we have not used the term “spectrum” when discussing the DTFT, but it should be clear at this point that it is appropriate to refer to the DTFT as a spectrum representation of a discrete-time signal. Recall that we introduced the term spectrum in Chapter 3 to mean the collection of frequency and complex amplitude information required to synthesize a signal using the Fourier synthesis equation in (3.26) in Section 3-5. In the case of the DTFT, the synthesis equation is the inverse transform integral (7.8), and the analysis equation (7.2) provides a means for determining the complex amplitudes of the complex exponentials $e^{j\hat{\omega}n}$ in the synthesis equation. To make this a little more concrete, we can

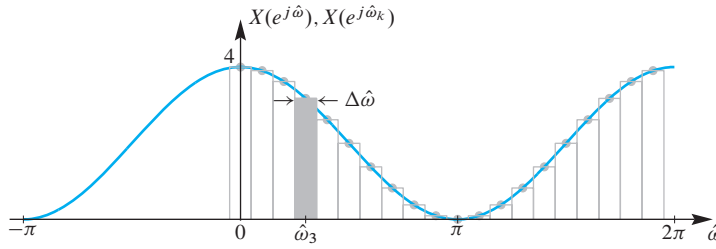


Figure 7-2 Riemann sum approximation to the integral of the inverse DTFT. Here, $X(e^{j\hat{\omega}}) = 2(1 + \cos \hat{\omega})$, which is the DTFT of $x[n] = \delta[n + 1] + 2\delta[n] + \delta[n - 1]$.

view the inverse DTFT integral as the limit of a finite sum by writing (7.8) in terms of the Riemann sum definition⁴ of the integral

$$x[n] = \frac{1}{2\pi} \int_0^{2\pi} X(e^{j\hat{\omega}}) e^{j\hat{\omega}n} d\hat{\omega} = \lim_{\Delta\hat{\omega} \rightarrow 0} \sum_{k=0}^{N-1} \left(\frac{1}{2\pi} X(e^{j\hat{\omega}_k}) \Delta\hat{\omega} \right) e^{j\hat{\omega}_k n} \quad (7.17)$$

where $\Delta\hat{\omega} = 2\pi/N$ is the spacing between the frequencies $\hat{\omega}_k = 2\pi k/N$, with the range of integration⁵ $0 \leq \hat{\omega} < 2\pi$ being covered by choosing $k = 0, 1, \dots, N - 1$. The expression on the right in (7.17) contains a *sum of complex exponential signals* whose spectrum representation is the set of frequencies $\hat{\omega}_k$ together with the corresponding complex amplitudes $X(e^{j\hat{\omega}_k}) \Delta\hat{\omega}/(2\pi)$. This is illustrated in Fig. 7-2 which shows the values $X(e^{j\hat{\omega}_k})$ as gray dots and the rectangles have area equal to $X(e^{j\hat{\omega}_k}) \Delta\hat{\omega}$. Each one of the rectangles can be viewed as a spectrum line, especially when $\Delta\hat{\omega} \rightarrow 0$. In the limit as $\Delta\hat{\omega} \rightarrow 0$, the magnitudes of the spectral components become infinitesimally small, as does the spacing between frequencies. Therefore, (7.17) suggests that the inverse DTFT integral synthesizes the signal $x[n]$ as a sum of infinitely small complex exponentials with all frequencies $0 \leq \hat{\omega} < 2\pi$ being used in the sum. The changing magnitude of $X(e^{j\hat{\omega}})$ specifies the relative amount of each frequency component that is required to synthesize $x[n]$. This is entirely consistent with the way we originally defined and subsequently used the concept of spectrum in Chapters 3–6, so we henceforth feel free to apply the term *spectrum* also to the DTFT representation.

7-2 Properties of the DTFT

We have motivated our study of the DTFT primarily by considering the problem of determining the frequency response of a filter, or more generally the Fourier representation of a signal. While these are important applications of the DTFT, it is also important to note that the DTFT also plays an important role as an “operator” in the theory of discrete-time signals and systems. This is best illustrated by highlighting some of the important properties of the DTFT operator.

⁴The Riemannsum approximation to an integral is $\int_0^u q(t)dt \approx \sum_{n=0}^{N_u-1} q(t_n)\Delta t$, where the integrand $q(t)$ is sampled at N_u equally spaced times $t_n = n\Delta t$, and $\Delta t = u/N_u$.

⁵We have used the result of Exercise 7.4 to change the limits to 0 to 2π .

7-2.1 Linearity Property

As we showed in Section 7-1.3, the DTFT operation obeys the principle of superposition (i.e., it is a linear operation). This is summarized in (7.18)

$$\boxed{x[n] = ax_1[n] + bx_2[n] \xleftrightarrow{\text{DTFT}} X(e^{j\hat{\omega}}) = aX_1(e^{j\hat{\omega}}) + bX_2(e^{j\hat{\omega}})} \quad (7.18)$$

7-2.2 Time-Delay Property

When we first studied sinusoids, the phase was shown to depend on the time-shift of the signal. The simple relationship was “phase equals the negative of frequency times time-shift.” This concept carries over to the general case of the Fourier transform. The time-delay property of the DTFT states that time-shifting results in a phase change in the frequency domain:

$$\boxed{y[n] = x[n - n_d] \xleftrightarrow{\text{DTFT}} Y(e^{j\hat{\omega}}) = X(e^{j\hat{\omega}})e^{-j\hat{\omega}n_d}} \quad (7.19)$$

The reason that the delay property is so important and useful is that (7.19) shows that multiplicative factors of the form $e^{-j\hat{\omega}n_d}$ in frequency-domain expressions always signify time delay.

EXAMPLE 7-3 Delayed Sinc Function

Let $y[n] = x[n - 10]$, where $x[n]$ is the sinc function of (7.13); that is,

$$y[n] = \frac{\sin \hat{\omega}_b(n - 10)}{\pi(n - 10)}$$

Using the time-delay property and the result for $X(e^{j\hat{\omega}})$ in (7.13), we can write down the following expression for the DTFT of $y[n]$ with virtually no further analysis:

$$Y(e^{j\hat{\omega}}) = X(e^{j\hat{\omega}})e^{-j\hat{\omega}10} = \begin{cases} e^{-j\hat{\omega}10} & 0 \leq |\hat{\omega}| \leq \hat{\omega}_b \\ 0 & \hat{\omega}_b < |\hat{\omega}| \leq \pi \end{cases}$$

Notice that the magnitude plot of $|Y(e^{j\hat{\omega}})|$ is still a rectangle as in Fig. 7-1(a); delay only changes the phase.

To prove the time-delay property, consider a sequence $y[n] = x[n - n_d]$, which we see is simply a time-shifted version of another sequence $x[n]$. We need to compare the DTFT of $y[n]$ vis-à-vis the DTFT of $x[n]$. By definition, the DTFT of $y[n]$ is

$$Y(e^{j\hat{\omega}}) = \sum_{n=-\infty}^{\infty} \underbrace{x[n - n_d]}_{y[n]} e^{-j\hat{\omega}n} \quad (7.20)$$

If we make the substitution $m = n - n_d$ for the index of summation in (7.20), we obtain

$$Y(e^{j\hat{\omega}}) = \sum_{m=-\infty}^{\infty} x[m]e^{-j\hat{\omega}(m+n_d)} = \sum_{m=-\infty}^{\infty} x[m]e^{-j\hat{\omega}m} e^{-j\hat{\omega}n_d} \quad (7.21)$$

Since the factor $e^{-j\hat{\omega}n_d}$ does not depend on m and is common to all the terms in the sum on the right in (7.21), we can write $Y(e^{j\hat{\omega}})$ as

$$Y(e^{j\hat{\omega}}) = \left(\sum_{m=-\infty}^{\infty} x[m]e^{-j\hat{\omega}m} \right) e^{-j\hat{\omega}n_d} = X(e^{j\hat{\omega}})e^{-j\hat{\omega}n_d} \quad (7.22)$$

Therefore, we have proved that time-shifting results in a phase change in the frequency domain.

7-2.3 Frequency-Shift Property

Consider a sequence $y[n] = e^{j\hat{\omega}_c n} x[n]$ where the DTFT of $x[n]$ is $X(e^{j\hat{\omega}})$. The multiplication by a complex exponential causes a frequency shift in the DTFT of $y[n]$ compared to the DTFT of $x[n]$. By definition, the DTFT of $y[n]$ is

$$Y(e^{j\hat{\omega}}) = \sum_{n=-\infty}^{\infty} \underbrace{e^{j\hat{\omega}_c n} x[n]}_{y[n]} e^{-j\hat{\omega}n} \quad (7.23)$$

If we combine the exponentials in the summation on the right side of (7.23), we obtain

$$Y(e^{j\hat{\omega}}) = \sum_{n=-\infty}^{\infty} x[n]e^{-j(\hat{\omega}-\hat{\omega}_c)n} = X(e^{j(\hat{\omega}-\hat{\omega}_c)}) \quad (7.24)$$

Therefore, we have proved the following general property of the DTFT:

Frequency-Shift Property of the DTFT

$$y[n] = e^{j\hat{\omega}_c n} x[n] \xleftrightarrow{\text{DTFT}} Y(e^{j\hat{\omega}}) = X(e^{j(\hat{\omega}-\hat{\omega}_c)}) \quad (7.25)$$

7-2.3.1 DTFT of a Complex Exponential

An excellent illustration of the frequency-shifting property comes from studying the DTFT of a finite-duration complex exponential. This is an important case for bandpass filter design and for spectrum analysis. In spectrum analysis, we would expect the DTFT to have a very large value at the frequency of the finite-duration complex exponential signal, and the frequency-shifting property makes it easy to see that fact.

Consider a length- L complex exponential signal

$$x_1[n] = Ae^{j(\hat{\omega}_0 n + \varphi)} \quad \text{for } n = 0, 1, 2, \dots, L-1$$

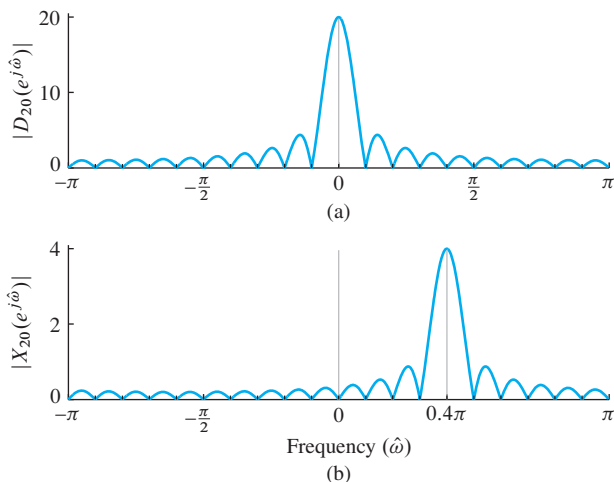


Figure 7-3 Illustration of DTFT frequency-shifting property. (a) DTFT magnitude for the length-20 rectangular window. (b) DTFT of a length-20 complex exponential with amplitude $A = 0.2$, and whose frequency is $\hat{\omega}_0 = 0.4\pi$.

which is zero for $n < 0$ and $n \geq L$. An alternative representation for $x_1[n]$ is the product of a length- L rectangular pulse times the complex exponential.

$$x_1[n] = A e^{j\varphi} \underbrace{e^{j(\hat{\omega}_0 n)} r_L[n]}_{\text{frequency shift}}$$

where the rectangular pulse $r_L[n]$ is equal to one for $n = 0, 1, 2, \dots, L - 1$, and zero elsewhere.

To determine an expression for the DTFT of $x_1[n]$, we use the DTFT of $r_L[n]$ which is known to contain a Dirichlet form⁶ as in (7.5) (also see Table 7-1 on p. 270). Figure 7-3(a) shows the DTFT magnitude for a length-20 rectangular pulse (i.e., $|R_{20}(e^{j\hat{\omega}})| = |D_{20}(e^{j\hat{\omega}})|$). The peak value of the Dirichlet is at $\hat{\omega} = 0$, and there are zeros at integer multiples of $2\pi/20 = 0.1\pi$, when $L = 20$.

Then the DTFT of $x_L[n]$ is obtained with the frequency-shifting property:

$$X_1(e^{j\hat{\omega}}) = A e^{j\varphi} R_L(e^{j(\hat{\omega} - \hat{\omega}_0)}) \quad (7.26a)$$

$$= A e^{j\varphi} D_L(\hat{\omega} - \hat{\omega}_0) e^{-j(\hat{\omega} - \hat{\omega}_0)(L-1)/2} \quad (7.26b)$$

where $D_L(\hat{\omega} - \hat{\omega}_0)$ is a frequency-shifted version of the Dirichlet form

$$D_L(\hat{\omega}) = \frac{\sin(\hat{\omega}L/2)}{\sin(\hat{\omega}/2)} \quad (7.27)$$

Since the exponential terms in (7.26b) only contribute to the phase, this result says that the magnitude $|X_L(e^{j\hat{\omega}})| = A |D_L(\hat{\omega} - \hat{\omega}_0)|$ is a frequency-shifted Dirichlet that is scaled by A . For $\hat{\omega}_0 = 0.4\pi$, $A = 0.2$, and $L = 20$, the length-20 complex exponential, $x_{20}[n] = 0.2 \exp(j0.4\pi n) r_{20}[n]$ has the DTFT magnitude shown in Fig. 7-3(b). Notice that the peak of the shifted Dirichlet envelope is at the frequency of the complex exponential, $\hat{\omega}_0 = 0.4\pi$. The peak height is the product of the Dirichlet peak height and the amplitude of the complex exponential, $AL = (0.2)(20) = 4$.

⁶The Dirichlet form was first defined in Section 6-7 on p. 228.

7-2.3.2 DTFT of a Real Cosine Signal

A sinusoid is composed of two complex exponentials, so the frequency-shifting property would be applied twice to obtain the DTFT. Consider a length- L sinusoid

$$s_L[n] = A \cos(\hat{\omega}_0 n + \varphi) \quad \text{for } n = 0, 1, \dots, L - 1 \quad (7.28a)$$

which we can write as the sum of complex exponentials at frequencies $+\hat{\omega}_0$ and $-\hat{\omega}_0$ as follows:

$$s_L[n] = \frac{1}{2} A e^{j\varphi} e^{j\hat{\omega}_0 n} + \frac{1}{2} A e^{-j\varphi} e^{-j\hat{\omega}_0 n} \quad \text{for } n = 0, 1, \dots, L - 1 \quad (7.28b)$$

Using the linearity of the DTFT and (7.26b) for the two frequencies $\pm\hat{\omega}_0$ leads to the expression

$$\begin{aligned} S_L(e^{j\hat{\omega}}) &= \frac{1}{2} A e^{j\varphi} D_L(\hat{\omega} - \hat{\omega}_0) e^{-j(\hat{\omega} - \hat{\omega}_0)(L-1)/2} \\ &\quad + \frac{1}{2} A e^{-j\varphi} D_L(\hat{\omega} + \hat{\omega}_0) e^{-j(\hat{\omega} + \hat{\omega}_0)(L-1)/2} \end{aligned} \quad (7.29)$$

where the function $D_L(\hat{\omega})$ is the Dirichlet form in (7.27). In words, the DTFT is the sum of two Dirichlets: one shifted up to $+\hat{\omega}_0$ and the other down to $-\hat{\omega}_0$.

Figure 7-4 shows $|S_{20}(e^{j\hat{\omega}})|$ as a function of $\hat{\omega}$ for the case $\hat{\omega}_0 = 0.4\pi$ with $A = 0.2$ and $L = 20$. The DTFT magnitude exhibits its characteristic even symmetry, and the peaks of the DTFT occur near $\hat{\omega}_0 = \pm 0.4\pi$. Furthermore, the peak heights are equal to approximately $\frac{1}{2}AL$, which can be shown by evaluating (7.29) for $\hat{\omega}_0 = 0.4\pi$, and assuming that the value of $|S_{20}(e^{j\hat{\omega}_0})|$ is determined entirely by the first term in (7.29).

In Section 8-7, we will revisit the fact that isolated spectral peaks are often indicative of sinusoidal signal components. Knowledge that the peak height depends on both the amplitude A and the duration L is useful in interpreting spectrum analysis results for signals involving multiple frequencies.

7-2.4 Convolution and the DTFT

Perhaps the most important property of the DTFT concerns the DTFT of a sequence that is the discrete-time convolution of two sequences. The following property says that the DTFT *transforms convolution into multiplication*.

Convolution Property of the DTFT

$$y[n] = x[n] * h[n] \xleftrightarrow{\text{DTFT}} Y(e^{j\hat{\omega}}) = X(e^{j\hat{\omega}})H(e^{j\hat{\omega}}) \quad (7.30)$$

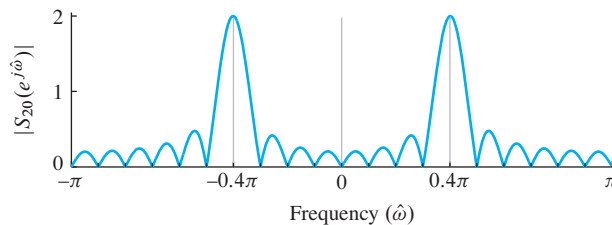


Figure 7-4 DTFT of a length-20 sinusoid with amplitude $A = 0.2$, and frequency $\hat{\omega}_0 = 0.4\pi$.

To illustrate the convolution property, consider the convolution of two signals $h[n] * x[n]$, where $x[n]$ a finite-length signal with three nonzero values

$$x[n] = 3\delta[n] + 4\delta[n - 1] + 5\delta[n - 2] \quad (7.31)$$

and $h[n]$ is a signal whose length may be finite or infinite. When the signal $x[n]$ is convolved with $h[n]$, we can write

$$\begin{aligned} y[n] &= \sum_{k=0}^M x[k]h[n - k] = x[0]h[n] + x[1]h[n - 1] \\ &\quad + x[2]h[n - 2] + \underbrace{x[3]h[n - 3] + \dots}_{\text{these terms are zero}} \end{aligned} \quad (7.32)$$

If we then take the DTFT of (7.32), we obtain

$$Y(e^{j\hat{\omega}}) = x[0]H(e^{j\hat{\omega}}) + x[1]e^{-j\hat{\omega}}H(e^{j\hat{\omega}}) + x[2]e^{-j2\hat{\omega}}H(e^{j\hat{\omega}}) \quad (7.33)$$

where the delay property applied to a term like $h[n - 2]$ creates the term $e^{-j2\hat{\omega}}H(e^{j\hat{\omega}})$. Then we observe that the term $H(e^{j\hat{\omega}})$ on the right-hand side of (7.33) can be factored out to write

$$Y(e^{j\hat{\omega}}) = \underbrace{(x[0] + x[1]e^{-j\hat{\omega}} + x[2]e^{-j2\hat{\omega}})}_{\text{DTFT of } x[n]} H(e^{j\hat{\omega}}) \quad (7.34a)$$

and, therefore, we have the desired result which is multiplication of the DTFTs as asserted in (7.30).

$$Y(e^{j\hat{\omega}}) = H(e^{j\hat{\omega}})X(e^{j\hat{\omega}}) \quad (7.34b)$$

Filling in the signal values for $x[n]$ in this example we obtain

$$Y(e^{j\hat{\omega}}) = X(e^{j\hat{\omega}})H(e^{j\hat{\omega}}) = \underbrace{(3 + 4e^{-j\hat{\omega}} + 5e^{-j2\hat{\omega}})}_{\text{coefficients are signal values}} H(e^{j\hat{\omega}}) \quad (7.34c)$$

The steps above do not depend on the numerical values of the signal $x[n]$, so a general proof could be constructed along these lines. In fact, the proof would be valid for signals of infinite length, where the limits on the sum in (7.32) would be infinite. The only additional concern for the infinite-length case would be that the DTFTs $X(e^{j\hat{\omega}})$ and $H(e^{j\hat{\omega}})$ must exist as we have discussed before.

EXAMPLE 7-4 Frequency Response of Delay

The delay property is a special case of the convolution property of the DTFT. To see this, recall that we can represent delay as the convolution with a shifted impulse

$$y[n] = x[n] * \delta[n - n_d] = x[n - n_d]$$

so the impulse response of a delay system is $h[n] = \delta[n - n_d]$. The corresponding frequency response (i.e., DTFT) of the delay system is

$$H(e^{j\hat{\omega}}) = \sum_{n=-\infty}^{\infty} \delta[n - n_d] e^{-j\hat{\omega}n} = e^{-j\hat{\omega}n_d}$$

Therefore, using the convolution property, the DTFT of the output of the delay system is

$$Y(e^{j\hat{\omega}}) = X(e^{j\hat{\omega}})H(e^{j\hat{\omega}}) = X(e^{j\hat{\omega}})e^{-j\hat{\omega}n_d}$$

which is identical to the delay property of (7.19).

7-2.4.1 Filtering is Convolution

The convolution property of LTI systems provides an effective way to think about LTI systems. In particular, when we think of LTI systems as “filters” we are thinking of their frequency responses, which can be chosen so that some frequencies of the input are blocked while others pass through with little modification. As we discussed in Section 7-1.11, the DTFT $X(e^{j\hat{\omega}})$ plays the role of spectrum for both finite-length signals and infinite-length signals. The convolution property (7.30) reinforces this view. If we use (7.30) to write the expression for the output of an LTI system using the DTFT synthesis integral, we have

$$y[n] = \frac{1}{2\pi} \int_0^{2\pi} H(e^{j\hat{\omega}}) X(e^{j\hat{\omega}}) e^{j\hat{\omega}n} d\hat{\omega} \quad (7.35a)$$

which can be approximated with a Riemann sum as in Section 7-1.11

$$y[n] = \lim_{\Delta\hat{\omega} \rightarrow 0} \sum_{k=0}^{N-1} H(e^{j\hat{\omega}_k}) \left(\frac{\Delta\hat{\omega}}{2\pi} X(e^{j\hat{\omega}_k}) \right) e^{j\hat{\omega}_k n} \quad (7.35b)$$

Now we see that the complex amplitude $\frac{\Delta\hat{\omega}}{2\pi} X(e^{j\hat{\omega}_k})$ at each frequency is modified by the frequency response $H(e^{j\hat{\omega}_k})$ of the system evaluated at the given frequency $\hat{\omega}_k$. This is exactly the same result as the *sinusoid-in gives sinusoid-out* property that we saw in Chapter 6 for case where the input is a discrete sum of complex exponentials. In Section 7-3, we will expand on this idea and define several ideal frequency-selective filters whose frequency responses are ideal versions of filters that we might want to implement in a signal processing application.

7-2.5 Energy Spectrum and the Autocorrelation Function

An important result in Fourier transform theory is *Parseval's Theorem*:

Parseval's Theorem for the Energy of a Signal

$$\sum_{n=-\infty}^{\infty} |x[n]|^2 = \frac{1}{2\pi} \int_{-\pi}^{\pi} |X(e^{j\hat{\omega}})|^2 d\hat{\omega} \quad (7.36)$$

The left-hand side of (7.36) is called the energy in the signal; it is a scalar. Thus, the right-hand side of (7.36) is also the energy, but the DTFT $|X(e^{j\hat{\omega}})|^2$ shows how the energy is distributed versus frequency. Therefore, the DTFT $|X(e^{j\hat{\omega}})|^2$ is called the *magnitude-squared spectrum* or the *energy spectrum* of $x[n]$.⁷ If we first define the energy of a signal as the sum of the squares

$$E = \sum_{n=-\infty}^{\infty} |x[n]|^2 \quad (7.37)$$

then the energy E is a single number that is often a convenient measure of the size of the signal.

EXAMPLE 7-5 Energy of the Sinc Signal

The energy of the sinc signal (evaluated in the time domain) is

$$E = \sum_{n=-\infty}^{\infty} \left(\frac{\sin \hat{\omega}_b n}{\pi n} \right)^2$$

While it is impossible to evaluate this sum directly, application of Parseval's theorem yields

$$E = \sum_{n=-\infty}^{\infty} \left(\frac{\sin \hat{\omega}_b n}{\pi n} \right)^2 = \frac{1}{2\pi} \int_{-\hat{\omega}_b}^{\hat{\omega}_b} |1|^2 d\hat{\omega} = \frac{\hat{\omega}_b}{\pi}$$

because the DTFT of the sinc signal is one for $-\hat{\omega}_b \leq \hat{\omega} \leq \hat{\omega}_b$. A simple interpretation of this result is that the energy is proportional to the bandwidth of the sinc signal and evenly distributed in $\hat{\omega}$ across the band $|\hat{\omega}| \leq \hat{\omega}_b$.

7-2.5.1 Autocorrelation Function

The energy spectrum is the Fourier transform of a time-domain signal which turns out to be the autocorrelation of $x[n]$. The autocorrelation function is widely used in signal detection applications. Its usual definition (7.39) is equivalent to the following convolution operation:

$$c_{xx}[n] = x[-n] * x[n] = \sum_{k=-\infty}^{\infty} x[-k]x[n-k] \quad (7.38)$$

By making the substitution $m = -k$ for the dummy index of summation, we can write

$$c_{xx}[n] = \sum_{m=-\infty}^{\infty} x[m]x[n+m] \quad -\infty < n < \infty \quad (7.39)$$

⁷In many physical systems, energy is calculated by taking the square of a physical quantity (like voltage) and integrating, or summing, over time.

which is the basic definition of the autocorrelation function when $x[n]$ is real. Observe that in (7.39), the index n serves to shift $x[n+m]$ with respect to $x[m]$ when both sequences are thought of as functions of m . It can be shown that $c_{xx}[n]$ is maximum at $n = 0$; because then $x[n+m]$ is perfectly aligned with $x[m]$. The independent variable n in $c_{xx}[n]$ is often called the “lag” by virtue of its meaning as a shift between two copies of the same sequence $x[n]$. When the lag is zero ($n = 0$) in (7.39), the value of the autocorrelation is equal to the energy in the signal (i.e., $E = c_{xx}[0]$).

EXERCISE 7.5

In (7.38), we use the time-reversed signal $x[-n]$. Show that the DTFT of $x[-n]$ is $X(e^{-j\hat{\omega}})$.

EXERCISE 7.6

In Chapter 6, we saw that the frequency response for a real impulse response must be conjugate symmetric. Since the frequency response function is a DTFT, it must also be true that the DTFT of a real signal $x[n]$ is conjugate symmetric. Show that if $x[n]$ is real, $X(e^{-j\hat{\omega}}) = X^*(e^{j\hat{\omega}})$.

Using the results of Exercises 7.5 and 7.6 for real signals, the DTFT of the autocorrelation function $c_{xx}[n] = x[-n] * x[n]$ is

$$C_{xx}(e^{j\hat{\omega}}) = X(e^{-j\hat{\omega}})X(e^{j\hat{\omega}}) = X^*(e^{j\hat{\omega}})X(e^{j\hat{\omega}}) = |X(e^{j\hat{\omega}})|^2 \quad (7.40)$$

Since $C_{xx}(e^{j\hat{\omega}})$ can be written as a magnitude squared, it is purely real and $C_{xx}(e^{j\hat{\omega}}) \geq 0$. A useful relationship results if we represent $c_{xx}[n]$ in terms of its inverse DTFT; that is,

$$c_{xx}[n] = \frac{1}{2\pi} \int_{-\pi}^{\pi} |X(e^{j\hat{\omega}})|^2 e^{j\hat{\omega}n} d\hat{\omega} \quad (7.41)$$

If we evaluate both sides of (7.41) at $n = 0$, we see that the energy of the sequence can also be computed from $C_{xx}(e^{j\hat{\omega}}) = |X(e^{j\hat{\omega}})|^2$ as follows:

$$E = c_{xx}[0] = \sum_{m=-\infty}^{\infty} |x[m]|^2 = \frac{1}{2\pi} \int_{-\pi}^{\pi} |X(e^{j\hat{\omega}})|^2 d\hat{\omega} \quad (7.42)$$

Finally, equating (7.37) and (7.42) we obtain *Parseval's Theorem* (7.36).

7-3 Ideal Filters

In any practical application of LTI discrete-time systems, the frequency response function $H(e^{j\hat{\omega}})$ would be derived by a filter design procedure that would yield an LTI system that could be implemented with finite computation. However, in the early phases of the system design process it is common practice to start with *ideal filters* that have simple frequency responses that provide ideal frequency selectivity.

7-3.1 Ideal Lowpass Filter

An ideal lowpass filter (LPF) has a frequency response that consists of two regions: the passband near $\hat{\omega} = 0$ (DC), where the frequency response is one, and the stopband away from $\hat{\omega} = 0$, where it is zero. An ideal LPF is therefore defined as

$$H_{\text{LP}}(e^{j\hat{\omega}}) = \begin{cases} 1 & |\hat{\omega}| \leq \hat{\omega}_{\text{co}} \\ 0 & \hat{\omega}_{\text{co}} < |\hat{\omega}| \leq \pi \end{cases} \quad (7.43)$$

The frequency $\hat{\omega}_{\text{co}}$ is called the *cutoff frequency* of the LPF passband. Figure 7-5 shows a plot of $H_{\text{LP}}(e^{j\hat{\omega}})$ for the ideal LPF. The shape is rectangular and $H_{\text{LP}}(e^{j\hat{\omega}})$ is even symmetric about $\hat{\omega} = 0$. As discussed in Section 6-4.3, this property is needed because real-valued impulse responses lead to filters with a conjugate symmetric frequency responses. Since $H_{\text{LP}}(e^{j\hat{\omega}})$ has zero phase, it is real-valued, so being conjugate symmetric is equivalent to being an even function.

EXERCISE 7.7

In Chapter 6, we saw that the frequency response for a real impulse response must be conjugate symmetric. Show that a frequency response defined with linear phase

$$H(e^{j\hat{\omega}}) = e^{-j7\hat{\omega}} H_{\text{LP}}(e^{j\hat{\omega}})$$

is conjugate symmetric, which would imply that its inverse DTFT is real.

The impulse response of the ideal LPF, found by applying the DTFT pair in (7.13), is a sinc function form

$$h_{\text{LP}}[n] = \frac{\sin \hat{\omega}_{\text{co}} n}{\pi n} \quad -\infty < n < \infty \quad (7.44)$$

The ideal LPF is impossible to implement because the impulse response $h_{\text{LP}}[n]$ is non-causal and, in fact, has nonzero values for large negative indices as well as large positive indices. However, that does not invalidate the ideal LPF concept; which is, the idea of selecting the low-frequency band and rejecting all other frequency components. Even the moving average filter discussed in Section 6-7.3 might be a satisfactory LPF in some applications. Figure 7-6 shows the frequency response of an 11-point moving average filter. Note that this causal filter has a lowpass-like frequency response magnitude, but

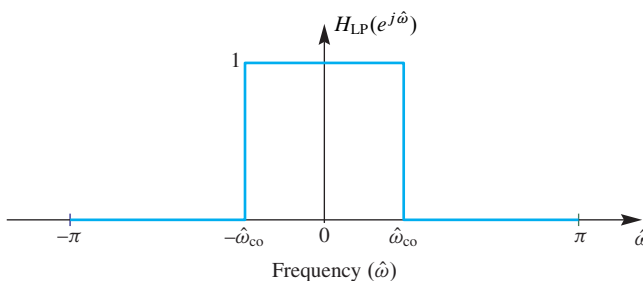


Figure 7-5 Frequency response of an ideal LPF with its cutoff at $\hat{\omega}_{\text{co}}$ rad/s. Recall that $H_{\text{LP}}(e^{j\hat{\omega}})$ must also be periodic with period 2π .

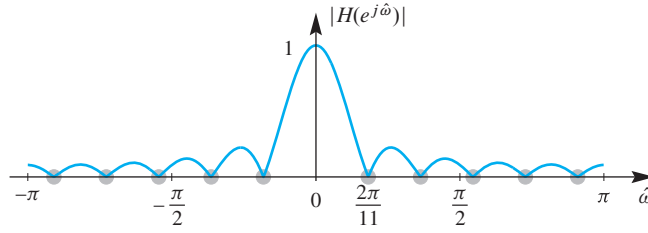


Figure 7-6 Magnitude response of an 11-point moving average filter. (Also shown in full detail in Fig. 6-8.)

it is far away from zero in what might be considered the stopband. In more stringent filtering applications, we need better approximations to the ideal characteristic. In a practical application, the process of filter design involves mathematical approximation of the ideal filter with a frequency response that is close enough to the ideal frequency response while corresponding to an implementable filter.

The following example shows the power of the transform approach when dealing with filtering problems.

EXAMPLE 7-6 Ideal Lowpass Filtering

Consider an ideal LPF with frequency response given by (7.43) and impulse response in (7.44). Now suppose that the input signal $x[n]$ to the ideal LPF is a bandlimited sinc signal

$$x[n] = \frac{\sin \hat{\omega}_b n}{\pi n} \quad (7.45)$$

Working in the time domain, the corresponding output of the ideal LPF would be given by the convolution expression

$$y[n] = x[n] * h_{\text{LP}}[n] = \sum_{m=-\infty}^{\infty} \left(\frac{\sin \hat{\omega}_b m}{\pi m} \right) \left(\frac{\sin \hat{\omega}_{\text{co}}(n-m)}{\pi(n-m)} \right) \quad -\infty < n < \infty \quad (7.46)$$

Evaluating this convolution directly in the time domain is impossible both analytically and via numerical computation. However, it is straightforward to obtain the filter output if we use the DTFT because in the frequency domain the transforms are rectangles and they are multiplied. From (7.13), the DTFT of the input is

$$X(e^{j\hat{\omega}}) = \begin{cases} 1 & |\hat{\omega}| \leq \hat{\omega}_b \\ 0 & \hat{\omega}_b < |\hat{\omega}| \leq \pi \end{cases} \quad (7.47)$$

Therefore, the DTFT of the ideal filter's output is $Y(e^{j\hat{\omega}}) = X(e^{j\hat{\omega}})H(e^{j\hat{\omega}})$, which would be of the form

$$Y(e^{j\hat{\omega}}) = X(e^{j\hat{\omega}})H_{\text{LP}}(e^{j\hat{\omega}}) = \begin{cases} 1 & |\hat{\omega}| \leq \hat{\omega}_a \\ 0 & \hat{\omega}_a < |\hat{\omega}| \leq \pi \end{cases} \quad (7.48a)$$

When multiplying the DTFTs to get the right-hand side of (7.48a), the product of the two rectangles is another rectangle whose width is the smaller of $\hat{\omega}_b$ and $\hat{\omega}_{co}$, so the bandlimit frequency $\hat{\omega}_a$ is

$$\hat{\omega}_a = \min(\hat{\omega}_b, \hat{\omega}_{co}) \quad (7.48b)$$

Since we want to determine the output signal $y[n]$, we must take the inverse DTFT of $Y(e^{j\hat{\omega}})$. Thus, using (7.13) to do the inverse transformation, the convolution in (7.46) evaluates to another sinc signal

$$y[n] = \sum_{m=-\infty}^{\infty} \left(\frac{\sin \hat{\omega}_b m}{\pi m} \right) \left(\frac{\sin \hat{\omega}_{co}(n-m)}{\pi(n-m)} \right) = \frac{\sin \hat{\omega}_a n}{\pi n} \quad -\infty < n < \infty \quad (7.49)$$

EXERCISE 7.8

The result given (7.48a) and (7.48b) is easily seen from a graphical solution that shows the rectangular shapes of the DTFTs. With $\hat{\omega}_b = 0.4\pi$ and $\hat{\omega}_{co} = 0.25\pi$, sketch plots of $X(e^{j\hat{\omega}})$ from (7.47) and $H_{LP}(e^{j\hat{\omega}})$ in (7.43) on the same set of axes and then verify the result in (7.48b).

We can generalize the result of Example 7-6 in several interesting ways. First, when $\hat{\omega}_b > \hat{\omega}_{co}$ we can see that the output is the impulse response of the ideal LPF, so the input (7.45) in a sense acts like an impulse to the ideal LPF. Furthermore, for ideal filters where a band of frequencies is completely removed by the filter, many different inputs could produce the same output. Also, we can see that if the bandlimit $\hat{\omega}_b$ of the input to an ideal LPF is less than the cutoff frequency (i.e., $\hat{\omega}_b \leq \hat{\omega}_{LP}$), then the input signal passes through the filter unchanged. Finally, if the input consists of a desired bandlimited signal plus some sort of competing signal such as noise whose spectrum extends over the entire range $|\hat{\omega}| \leq \pi$, then if the signal spectrum is concentrated in a band $|\hat{\omega}| \leq \hat{\omega}_b$, it follows by the principle of superposition that an ideal LPF with cutoff frequency $\hat{\omega}_{co} = \hat{\omega}_b$ passes the desired signal without modification while removing all frequencies in the spectrum of the competing signal above the cutoff frequency. This is often the motivation for using a LPF.

7-3.2 Ideal Highpass Filter

The ideal highpass filter (HPF) has its stopband centered on low frequencies, and its passband extends from $|\hat{\omega}| = \hat{\omega}_{co}$ out to $|\hat{\omega}| = \pi$. (The highest normalized frequency in a sampled signal is of course π .)

$$H_{HP}(e^{j\hat{\omega}}) = \begin{cases} 0 & |\hat{\omega}| \leq \hat{\omega}_{co} \\ 1 & \hat{\omega}_{co} < |\hat{\omega}| \leq \pi \end{cases} \quad (7.50)$$

Figure 7-7 shows an ideal HPF with its cutoff frequency at $\hat{\omega}_{co}$ rad/s. In this case, the high frequency components of a signal pass through the filter unchanged while the low

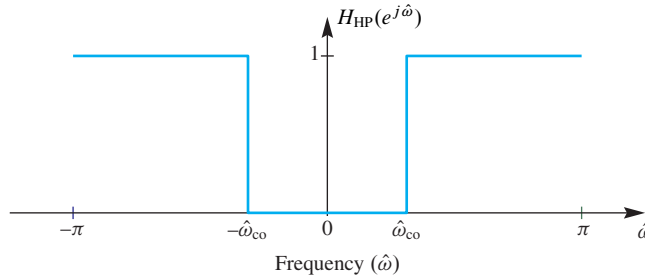


Figure 7-7 Frequency response of an ideal HPF with cutoff at $\hat{\omega}_{co}$ rad/s.

frequency components are completely eliminated. Highpass filters are often used to remove constant levels (DC) in sampled signals. Like the ideal LPF, we should define the ideal highpass filter with conjugate symmetry $H_{HP}(e^{-j\hat{\omega}}) = H_{HP}^*(e^{j\hat{\omega}})$ so that the corresponding impulse response is a real function of time.

EXERCISE 7.9

If $H_{LP}(e^{j\hat{\omega}})$ is an ideal LPF with its cutoff frequency at $\hat{\omega}_{co}$ as plotted in Fig. 7-5, show that the frequency response of an ideal HPF with cutoff frequency $\hat{\omega}_{co}$ can be represented by

$$H_{HP}(e^{j\hat{\omega}}) = 1 - H_{LP}(e^{j\hat{\omega}})$$

Hint: Try plotting the function $1 - H_{LP}(e^{j\hat{\omega}})$.

EXERCISE 7.10

Using the results of Exercise 7.9, show that the impulse response of the ideal HPF is

$$h_{HP}[n] = \delta[n] - \frac{\sin(\hat{\omega}_{co}n)}{\pi n}$$

7-3.3 Ideal Bandpass Filter

The ideal bandpass filter (BPF) has a passband centered away from the low-frequency band, so it has two stopbands, one near DC and the other at high frequencies. Two cutoff frequencies must be given to specify the ideal BPF, $\hat{\omega}_{co1}$ for the lower cutoff, and $\hat{\omega}_{co2}$ for the upper cutoff. That is, the ideal BPF has frequency response

$$H_{BP}(e^{j\hat{\omega}}) = \begin{cases} 0 & |\hat{\omega}| < \hat{\omega}_{co1} \\ 1 & \hat{\omega}_{co1} \leq |\hat{\omega}| \leq \hat{\omega}_{co2} \\ 0 & \hat{\omega}_{co2} < |\hat{\omega}| \leq \pi \end{cases} \quad (7.51)$$

Figure 7-8 shows an ideal BPF with its cutoff frequencies at $\hat{\omega}_{co1}$ and $\hat{\omega}_{co2}$. Once again we use a symmetrical definition of the passbands and stopbands which is required to make the corresponding impulse response real. In this case, all frequency components

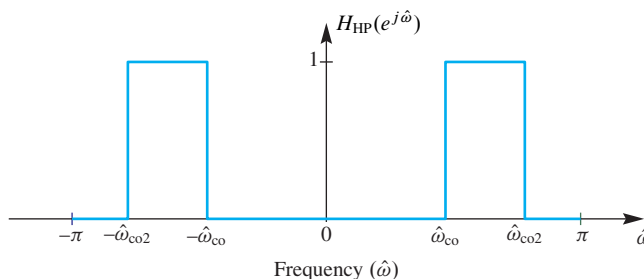


Figure 7-8 Frequency response of an ideal BPF with its passband from $\hat{\omega} = \hat{\omega}_{co1}$ to $\hat{\omega} = \hat{\omega}_{co2}$ rad/s.

of a signal that lie in the band $\hat{\omega}_{co1} \leq |\hat{\omega}| \leq \hat{\omega}_{co2}$ are passed unchanged through the filter, while all other frequency components are completely removed.

EXERCISE 7.11

If $H_{BP}(e^{j\hat{\omega}})$ is an ideal BPF with its cutoffs at $\hat{\omega}_{co1}$ and $\hat{\omega}_{co2}$, show by plotting that the filter defined by $H_{BR}(e^{j\hat{\omega}}) = 1 - H_{BP}(e^{j\hat{\omega}})$ could be called an ideal *band-reject* filter. Determine the edges of the stopband of the band-reject filter.

7-4 Practical FIR Filters

Ideal filters are useful concepts, but not practical since they cannot be implemented with a finite amount of computation. Therefore, we perform *filter design* to approximate an ideal frequency response to get a practical filter. For FIR filters, a filter design method must produce filter coefficients $\{b_k\}$ for the time-domain implementation of the FIR filter as a difference equation

$$y[n] = b_0x[n] + b_1x[n-1] + b_2x[n-2] + \cdots + b_Mx[n-M]$$

The filter coefficients are the values of the impulse response, and the DTFT of the impulse response determines the actual magnitude and phase of the designed frequency response, which can then be assessed to determine how closely it matches the desired ideal response. There are many ways to approximate the ideal frequency response, but we concentrate on the method of *windowing* which can be analyzed via the DTFT.

7-4.1 Windowing

The concept of windowing is widely used in signal processing. The basic idea is to *extract a finite section* of a very long signal $x[n]$ **via multiplication** $w[n]x[n+n_0]$. This approach works if the window function $w[n]$ is zero outside of a finite-length interval. In filter design the window *truncates* the infinitely long ideal impulse response $h_i[n]$,⁸ and then modify the truncated impulse response. The simplest window function is the *L*-point *rectangular window* which is the same as the rectangular pulse studied in Section 7-1.5.

$$w_r[n] = r_L[n] = \begin{cases} 1 & 0 \leq n \leq L-1 \\ 0 & \text{elsewhere} \end{cases} \quad (7.52)$$

⁸The subscript *i* denotes an ideal filter of the type discussed in Section 7-3.

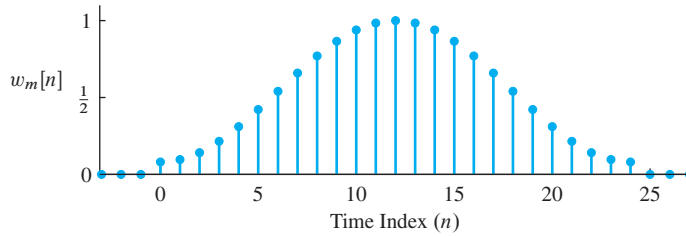


Figure 7-9 Length-21 Hamming window is nonzero only for $n = 0, 1, \dots, 20$.

Multiplying by a rectangular window only truncates a signal.

The important idea of windowing is that the product $w_r[n]h_i[n+n_0]$ extracts L values from the signal $h_i[n]$ starting at $n = n_0$. Thus, the following equation is equivalent

$$w_r[n]h_i[n+n_0] = \begin{cases} 0 & n < 0 \\ w_r[n]h_i[n+n_0] & 0 \leq n \leq L-1 \\ 0 & n \geq L \end{cases} \quad (7.53)$$

The name *window* comes from the idea that we can only “see” L values of the signal $h_i[n+n_0]$ within the window interval when we “look” through the window. Multiplying by $w[n]$ is looking through the window. When we change n_0 , the signal shifts, and we see a different length- L section of the signal.

The nonzero values of the window function do not have to be all ones, but they should be positive. For example, the symmetric L -point Hamming window⁹ is defined as

$$w_m[n] = \begin{cases} 0.54 - 0.46 \cos(2\pi n/(L-1)) & 0 \leq n \leq L-1 \\ 0 & \text{elsewhere} \end{cases} \quad (7.54)$$

The MATLAB function `hamming(L)` computes a vector with values given by (7.54). The stem plot of the Hamming window in Fig. 7-9 shows that the values are larger in the middle and taper off near the ends. The window length can be even or odd, but an odd-length Hamming window is easier to characterize. Its maximum value is 1.0 which occurs at the midpoint index location $n = (L-1)/2$, and the window is symmetric about the midpoint, with *even symmetry* because $w_m[n] = w_m[L-1-n]$.

7-4.2 Filter Design

Ideal Filters are given by their frequency response, consisting of *perfect* passbands and stopbands. The ideal filters cannot be FIR filters because there is no finite set of filter coefficients whose DTFT is equal to the ideal frequency response. Recall that the impulse response of the ideal LPF is an infinitely long sinc function as shown by the following DTFT pair:

$$h_i[n] = \frac{\sin(\hat{\omega}_c n)}{\pi n} \iff H_i(e^{j\hat{\omega}}) = \begin{cases} 1 & |\hat{\omega}| \leq \hat{\omega}_c \\ 0 & \hat{\omega}_c < |\hat{\omega}| \leq \pi \end{cases} \quad (7.55)$$

⁹This window is named for Richard Hamming who found that improved frequency-domain characteristics result from slight adjustments in the 0.5 coefficients in (8.49).

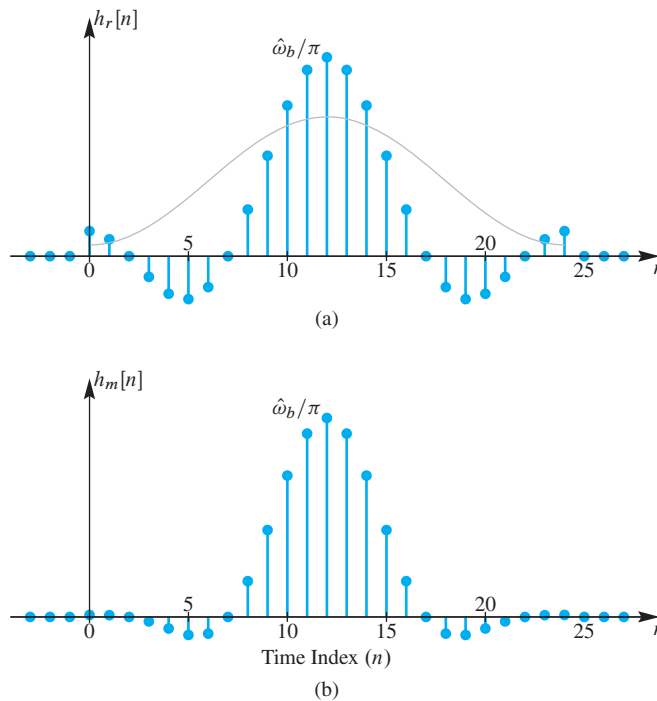


Figure 7-10 Impulse responses for two LPFs. (a) Length-25 LPF with rectangular window (i.e., truncated sinc function). (b) Length-25 LPF using 25-point Hamming window multiplying a sinc function. The shape of the Hamming window is shown in (a) because it truncates and multiplies the sinc function shown in (a).

where $\hat{\omega}_c$ is the *cutoff frequency* of the ideal LPF, which separates the passband from the stopband. The sinc function is infinitely long.

7-4.2.1 Window the Ideal Impulse Response

In order to make a practical FIR filter, we can multiply the sinc function by a window to produce a length- L impulse response. However, we must also shift the sinc function so that its main lobe is in the center of the window, because intuitively we should use the largest values from the ideal impulse response. From the shifting property of the DTFT, the time shift of $(L - 1)/2$ introduces a linear phase in the DTFT. Thus, the impulse response obtained from windowing is

$$\begin{aligned}
 h[n] &= w[n]h_i[n - (L - 1)/2] \\
 &= \begin{cases} w[n] \frac{\sin(\hat{\omega}_c(n - (L - 1)/2))}{\pi(n - (L - 1)/2)} & n = 0, 1, \dots, L - 1 \\ 0 & \text{elsewhere} \end{cases} \quad (7.56)
 \end{aligned}$$

where $w[n]$ is the window, either rectangular or Hamming.¹⁰ Since the nonzero domain of the window starts at $n = 0$, the resulting FIR filter is causal. We usually say that the practical FIR filter has an impulse response that is a *windowed* version of the ideal impulse response.

¹⁰We only consider rectangular and Hamming windows here, but there are many other window functions, and each of them results in filters with different frequency response characteristics.

The windowing operation is shown in Fig. 7-10(a) for the rectangular window which truncates the ideal impulse response to length- $L = 25$. In Fig. 7-10(b), the Hamming-windowed impulse response $h_m[n]$ results from truncating the ideal impulse response, and also weighting the values to reduce the ends more than the middle. The midpoint value is preserved (i.e., $h_m[12] = \hat{\omega}_c/\pi$) while the first and last points are 8% of their original values (e.g., $h_m[0] = 0.08h_i[0]$). A continuous outline of the Hamming window is drawn in (a) to show the weighting that is applied to the truncated ideal impulse response. The benefit of using the Hamming window comes from the fact that it smoothly tapers the ends of the truncated ideal lowpass impulse response.

7-4.2.2 Frequency Response of Practical Filters

A *practical filter* is a causal length- L filter whose frequency response closely approximates the desired frequency response of an ideal filter. Although it is possible to take the DTFT of a windowed sinc, the resulting formula is quite complicated and does not offer much insight into the quality of the frequency-domain approximation. Instead, we can evaluate the frequency response directly using MATLAB's `freqz` function because we have a simple formula for the windowed filter coefficients.

Figure 7-11(a) shows the magnitude response for an FIR filter whose impulse response is a length-25 truncated ideal impulse response with $\hat{\omega}_c = 0.4\pi$. The passband of the actual filter is not flat but it oscillates above and below the desired passband value of one; the same behavior is exhibited in the stopband. These *passband and stopband ripples*

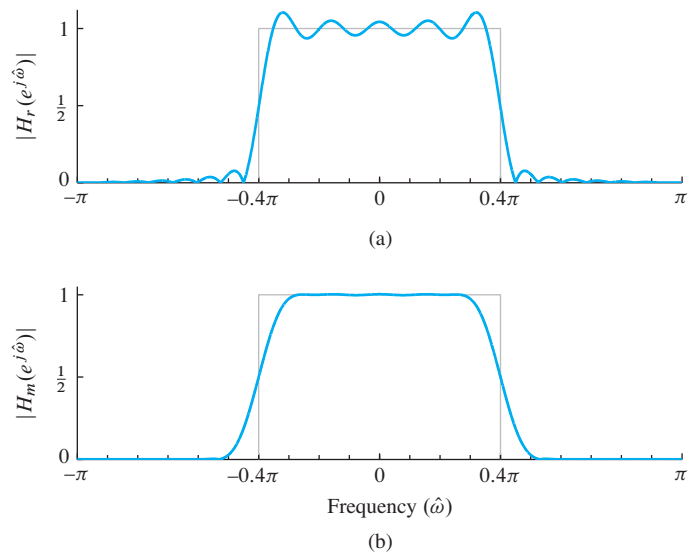


Figure 7-11 Frequency response magnitudes for LPFs whose impulse responses are shown in Fig. 7-10. (a) Length-25 LPF whose impulse response is a truncated sinc function obtained with a rectangular window. (b) Length-25 LPF whose impulse response is the product of a 25-point Hamming window and a sinc function. The ideal LPF with $\hat{\omega}_c = 0.4\pi$ is shown in gray. The phase response of both of these filters is a linear phase with slope $-(L - 1)/2 = -12$.

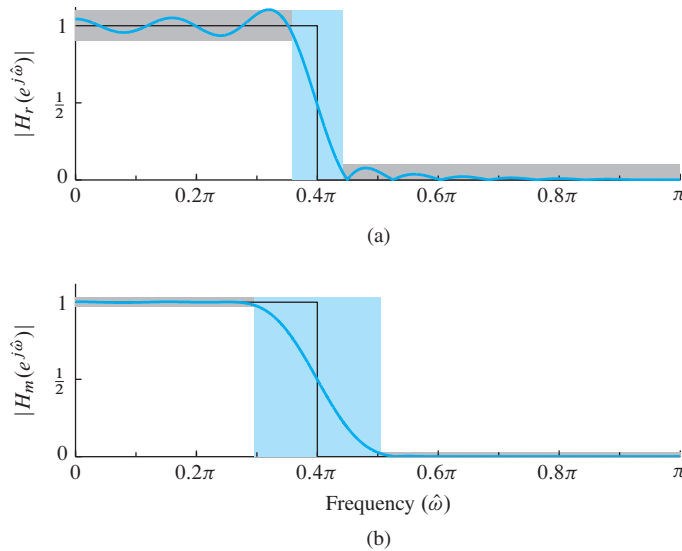


Figure 7-12 LPF template showing passband and stopband ripple tolerances along with the transition zone. (a) Length-25 LPF with rectangular window (i.e., truncated sinc). (b) Length-25 LPF using 25-point Hamming window. Only the positive half of the frequency axis is shown, because the magnitude response is an even function whenever the impulse response is real.

are usually observed for practical FIR filters that approximate ideal LPFs, and they are particularly noticeable with the rectangular window.

Figure 7-11(b) shows the magnitude response for an FIR filter whose impulse response is a length-25 Hamming-windowed sinc. In this case, the ripples are not visible on the magnitude plot because the scale is linear and the ripples are tiny, less than 0.0033. In terms of approximating the value of one in the passband and zero in the stopband, the Hamming-windowed ideal LPF is much better. However, this improved approximation comes at a cost—the edge of the passband near the cutoff frequency has a much lower slope. In filter design, we usually say it “falls off more slowly” from the passband to the stopband. Before we can answer the question of which filter is better, we must decide whether ripples are more important than the fall off rate from passband to stopband, or vice versa.

7-4.2.3 Passband Defined for the Frequency Response

Frequency-selective digital filters (e.g., LPFs, BPFs, and HPFs) have a magnitude response that is close to one in some frequency regions, and close to zero in others. For example, the plot in Fig. 7-12(a) is an LPF whose magnitude is within (approximately) $\pm 10\%$ of one when $0 \leq \hat{\omega} < 0.364\pi$. This region where the magnitude is close to one is called the *passband* of the filter. It is useful to have a precise definition of the passband edges, so that the passband width can be measured and we can compare different filters.

From a plot of the magnitude response (e.g, via `freqz` in MATLAB) it is possible to determine the set of frequencies where the magnitude is very close to one, as defined by $||H(e^{j\hat{\omega}})| - 1|$ being less than δ_p , which is called the *passband ripple*. A common design choice for the desired passband ripple is a value between 0.01 and 0.1 (i.e., 1% to

10%). For a LPF, the passband region extends from $\hat{\omega} = 0$ to $\hat{\omega}_p$, where the parameter $\hat{\omega}_p$ is called the *passband edge*.

For the two LPFs shown in Fig. 7-12, we can make an accurate measurement of δ_p and $\hat{\omega}_p$ from the zoomed plots in Fig. 7-13. For the rectangular window case, a careful measurement gives a maximum passband ripple size of $\delta_p = 0.104$, with the passband edge at $\hat{\omega}_p = 0.364\pi$. For the Hamming window case, we need the zoomed plot of the passband region to see the ripples, as in Fig. 7-13(b). Then we can measure the passband ripple to be $\delta_p = 0.003$ for the Hamming window case—more than 30 times smaller. Once we settle on the passband ripple height, we can measure the passband edge; in Fig. 7-12(b) it is $\hat{\omega}_p = 0.2596\pi$. Notice that the *actual passband edges* are not equal to the design parameter $\hat{\omega}_c$ which is called the *cutoff frequency*. There is sometimes a confusion when the terminology “passband cutoff frequency” is used to mean passband edge, which then implies that $\hat{\omega}_c$ and $\hat{\omega}_p$ might be the same, but after doing a few examples it should become clear that this is never the case.

7-4.2.4 Stopband Defined for the Frequency Response

When the frequency response (magnitude) of the digital filter is close to zero, we have the *stopband* region of the filter. The stopband is a region of the form $\hat{\omega}_s \leq \hat{\omega} \leq \pi$, if the magnitude response of a LPF is plotted only for nonnegative frequencies. The parameter $\hat{\omega}_s$ is called the *stopband edge*. In the rectangular window LPF example of Figs. 7-12(a) and 7-13(a), the magnitude is close to zero when $0.438\pi \leq \hat{\omega} \leq \pi$ (i.e.,

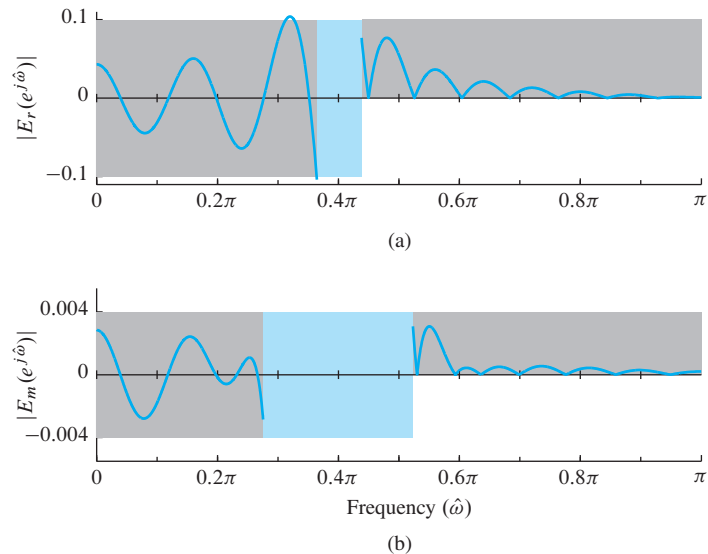


Figure 7-13 Blowup of the error between the actual magnitude response and the ideal, $E(e^{j\hat{\omega}}) = |H(e^{j\hat{\omega}})| - |H_i(e^{j\hat{\omega}})|$, which shows the passband and stopband ripples. (a) Length-25 LPF $H_r(e^{j\hat{\omega}})$ with rectangular window (i.e., truncated ideal lowpass impulse response). (b) Length-25 LPF $H_m(e^{j\hat{\omega}})$ using 25-point Hamming window. The ripples for the Hamming case are more than 30 times smaller.

high frequencies). The stopband ripple for this region is expected to be less than 0.1, and is measured to be $\delta_s = 0.077$. For the rectangular windowed sinc, the stopband edge is $\hat{\omega}_s = 0.4383\pi$.

We can repeat this process for the Hamming window LPF using Figs. 7-12(b) and 7-13(b) to determine the stopband ripple δ_s , and then the set of frequencies where the magnitude is less than δ_s . The result is a stopband ripple measurement of 0.0033, and a corresponding stopband edge of $\hat{\omega}_s = 0.5361\pi$.

7-4.2.5 Transition Zone of the LPF

Unlike an ideal LPF where the stopband begins at the same frequency where the passband ends, in a practical filter there is always a nonzero difference between the passband edge and the stopband edge. This difference is called the *transition width* of the filter: $\Delta\hat{\omega} = \hat{\omega}_s - \hat{\omega}_p$. The smaller the transition width, the better the filter because it is closer to the *ideal filter* which has a transition width of zero.

For the LPFs in Fig. 7-12, the measured transition width of the rectangular windowed sinc is

$$\Delta\hat{\omega}_r = \hat{\omega}_s - \hat{\omega}_p = 0.4383\pi - 0.3646\pi = 0.0737\pi \quad (7.57a)$$

while the Hamming windowed sinc has a much wider transition width—almost four times wider

$$\Delta\hat{\omega}_m = \hat{\omega}_s - \hat{\omega}_p = 0.5361\pi - 0.2596\pi = 0.2765\pi \quad (7.57b)$$

EXAMPLE 7-7 Decrease Transition Width

One property of the transition width is that it can be controlled by changing the filter order. There is an approximate inverse relationship, so doubling the order reduces the transition width by roughly one half. We can test this idea on the length-25 rectangular window LPF in Fig. 7-12(b) which has an order equal to 24. If we design a new LPF that has the same cutoff frequency, $\hat{\omega}_c = 0.4\pi$, but twice the order (i.e., $M = 48$), then we can repeat the measurement of the bandedges $\hat{\omega}_p$, $\hat{\omega}_s$, and the transition width $\Delta\hat{\omega}$.

| Filter | Order: M | $\hat{\omega}_p$ | $\hat{\omega}_s$ | $\Delta\hat{\omega}$ |
|---------|------------|------------------|------------------|----------------------|
| Rect | 24 | 0.3646π | 0.4383π | 0.0737π |
| Rect | 48 | 0.3824π | 0.4192π | 0.0368π |
| Rect | 96 | 0.3909π | 0.4100π | 0.0191π |
| Hamming | 24 | 0.2596π | 0.5361π | 0.2765π |
| Hamming | 48 | 0.3308π | 0.4687π | 0.1379π |
| Hamming | 96 | 0.3660π | 0.4340π | 0.0680π |

Comparing the values of $\Delta\hat{\omega}$, the ratio is $(0.0737\pi)/(0.0368\pi) = 2.003$. Doubling the order once more to $M = 96$ gives a transition width of 0.0191π , so the ratio is $(0.0737\pi)/(0.0191\pi) = 3.86 \approx 4$. For the Hamming window case, the measured transition width for $M = 48$ is $\Delta\hat{\omega} = 0.1379\pi$, and for $M = 96$, $\Delta\hat{\omega} = 0.0680\pi$. The ratios of 0.2765π to 0.1379π and 0.0680π are 2.005 and 4.066 which matches the approximate inverse relationship expected.

When comparing the transition widths in (7.57a) and (7.57b), we see that $\Delta\hat{\omega}_m = 3.75\Delta\hat{\omega}_r$, so the transition width of the Hamming window LPF is almost four times larger for $L = 25$. This empirical observation confirms the statement, “when comparing equal-order FIR filters that approximate a LPF, the one with larger transition width has smaller ripples.” However, this statement does not mean that the ripples can be reduced merely by widening the transition width. Within one window type, such as Hamming window filters, changing the transition width does not change the ripples by more than a few percent.

7-4.2.6 Summary of Filter Specifications

The foregoing discussion of ripples, bandedges, and transition width can be summarized with the tolerance scheme shown in Fig. 7-12. The filter design process is to approximate the ideal frequency response very closely. Once we specify the desired ripples and bandedges, we can draw a template around the ideal frequency response. The template should, in effect, give the trade-off between ripple size and transition width. Then an acceptable filter design would be any FIR filter whose magnitude response lies entirely within the template. The Hamming window method is just one possible design method among many that have been developed.

7-4.3 GUI for Filter Design

The *DSP-First* GUI called **filterdesign** illustrates several filter design methods for LPF, BPF, and HPF filters. The interface is shown in Fig. 7-14. Both FIR and IIR filters can be designed, but we are only interested in the FIR case which is selected with the **FIR** button in the upper right. The default design method is the *Window Method* using a Hamming window. The window type can be changed by selecting another window type from the drop-down list in the lower right. To specify the design it is necessary to set the order of the FIR filter and choose one or more cutoff frequencies; these parameters can be entered in the edit boxes.

The plot initially shows the frequency response magnitude on a linear scale, with a frequency axis in Hz. Clicking on the word **Magnitude** toggles the magnitude scale to a log scale in dB. Clicking on the word **Frequency** toggles the frequency axis to normalized frequency $\hat{\omega}$, and also let you enter the cutoff frequency using $\hat{\omega}$. Recall

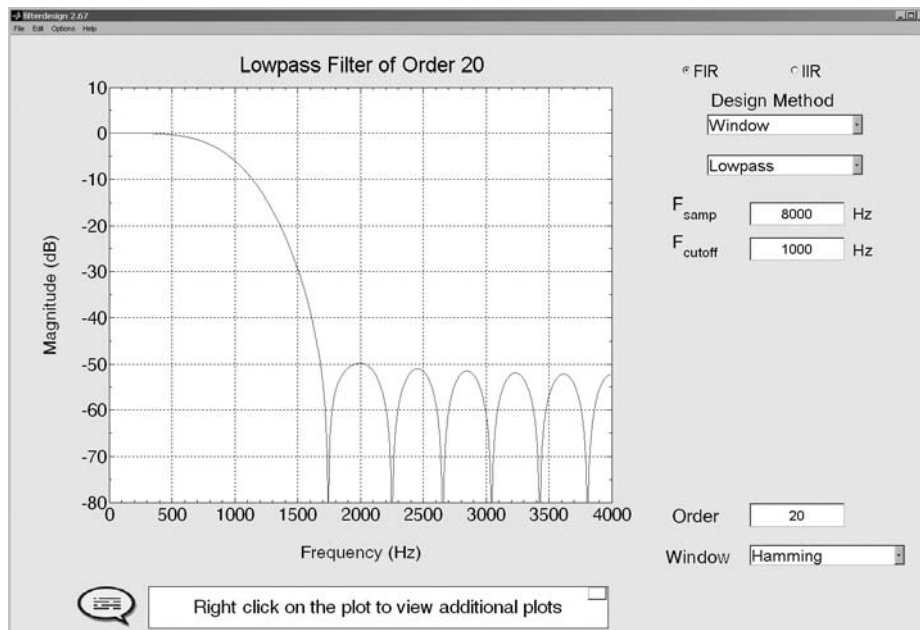


Figure 7-14 Interface for the `filterdesign` GUI. When the Filter Choice is set to FIR, many different window types can be selected, including the Hamming window and the Rectangular window (i.e., only truncation to a finite length). The specification of one or more cutoff frequencies (f_{co}) must be entered using continuous-time frequency (in Hz), along with a sampling rate (f_s , also in Hz). In normalized frequency, the cutoff frequency is $\hat{\omega}_{co} = 2\pi(f_{co}/f_s)$.

that $\hat{\omega} = 2\pi(f_{co}/f_s)$. The plotting region can also show the phase response of $H(e^{j\hat{\omega}})$, or the impulse response of the filter $h[n]$. Right click on the plot region to get a menu. The `Options` menu provides zooming and a grid via `Options->Zoom` and `Options->Grid`.

The filter coefficients can be “exported” from the GUI by using the menu `File->Export Coeffs`. To make some filters for comparison, redo the designs in Fig. 7-12 and export the filter coefficients to the workspace under unique names. Then you can make your own plot of the frequency response in MATLAB using the `freekz` function (or `freqz`) followed by a `plot` command. For example, an interesting activity would be to design the filters in Fig. 7-13 to check the measurements of ripples and transition width.

7-5 Table of Fourier Transform Properties and Pairs

Table 7-1 on p. 270 includes all the Fourier transform pairs that we have derived in this chapter as well as one pair (the left-sided exponential) that we did not derive. In addition, the basic properties of the Fourier transform, which make the DTFT convenient

to use in designing and analyzing systems, are given in Table 7-2 on p. 271 for easy reference.

7-6 Summary and Links

In this chapter, we introduced the DTFT, and developed some of its basic properties for understanding the behavior of linear systems. The DTFT provides a frequency-domain representation for signals as well as systems, and like other Fourier transforms it generalizes the idea of a spectrum for a discrete-time signal. We obtained the DTFT by generalizing the concept of the frequency response, and showed how the inverse transform could be used to obtain the impulse response of various ideal filters. Also it is not surprising that the DTFT plays an important role in filter design for methods based on rectangular and Hamming windowing.

Table 7-1 Basic discrete-time Fourier transform pairs.

| Table of DTFT Pairs | |
|--|---|
| <i>Time-Domain: $x[n]$</i> | <i>Frequency-Domain: $X(e^{j\hat{\omega}})$</i> |
| $\delta[n]$ | 1 |
| $\delta[n - n_d]$ | $e^{-j\hat{\omega}n_d}$ |
| $r_L[n] = u[n] - u[n - L]$ | $\frac{\sin(\frac{1}{2}L\hat{\omega})}{\sin(\frac{1}{2}\hat{\omega})} e^{-j\hat{\omega}(L-1)/2}$ |
| $r_L[n] e^{j\hat{\omega}_0 n}$ | $\frac{\sin(\frac{1}{2}L(\hat{\omega} - \hat{\omega}_0))}{\sin(\frac{1}{2}(\hat{\omega} - \hat{\omega}_0))} e^{-j(\hat{\omega} - \hat{\omega}_0)(L-1)/2}$ |
| $\frac{\sin(\hat{\omega}_b n)}{\pi n}$ | $\begin{cases} 1 & \hat{\omega} \leq \hat{\omega}_b \\ 0 & \hat{\omega}_b < \hat{\omega} \leq \pi \end{cases}$ |
| $a^n u[n] \quad (a < 1)$ | $\frac{1}{1 - ae^{-j\hat{\omega}}}$ |
| $-b^n u[-n - 1] \quad (b > 1)$ | $\frac{1}{1 - be^{-j\hat{\omega}}}$ |

Table 7-2 Basic discrete-time Fourier transform properties.

| Table of DTFT Properties | | |
|---------------------------------|--|---|
| Property Name | Time-Domain: $x[n]$ | Frequency-Domain: $X(e^{j\hat{\omega}})$ |
| Periodic in $\hat{\omega}$ | | $X(e^{j(\hat{\omega}+2\pi)}) = X(e^{j\hat{\omega}})$ |
| Linearity | $ax_1[n] + bx_2[n]$ | $aX_1(e^{j\hat{\omega}}) + bX_2(e^{j\hat{\omega}})$ |
| Conjugate Symmetry | $x[n]$ is real | $X(e^{-j\hat{\omega}}) = X^*(e^{j\hat{\omega}})$ |
| Conjugation | $x^*[n]$ | $X^*(e^{-j\hat{\omega}})$ |
| Time-Reversal | $x[-n]$ | $X(e^{-j\hat{\omega}})$ |
| Delay | $x[n - n_d]$ | $e^{-j\hat{\omega}n_d} X(e^{j\hat{\omega}})$ |
| Frequency Shift | $x[n]e^{j\hat{\omega}_0n}$ | $X(e^{j(\hat{\omega}-\hat{\omega}_0)})$ |
| Modulation | $x[n] \cos(\hat{\omega}_0n)$ | $\frac{1}{2}X(e^{j(\hat{\omega}-\hat{\omega}_0)}) + \frac{1}{2}X(e^{j(\hat{\omega}+\hat{\omega}_0)})$ |
| Convolution | $x[n] * h[n]$ | $X(e^{j\hat{\omega}})H(e^{j\hat{\omega}})$ |
| Autocorrelation | $x[-n] * x[n]$ | $ X(e^{j\hat{\omega}}) ^2$ |
| Parseval's Theorem | $\sum_{n=-\infty}^{\infty} x[n] ^2 = \frac{1}{2\pi} \int_{-\pi}^{\pi} X(e^{j\hat{\omega}}) ^2 d\hat{\omega}$ | |

7-7 Problems

P-7.1 Determine the DTFT of each of the following sequences:

(a) $x_1[n] = 2\delta[n - 3]$

(b) $x_2[n] = 3\delta[n - 2] - \delta[n - 3] + 3\delta[n - 4]$

$$(c) x_3[n] = 7u[n - 1] - 7u[n - 9]$$

$$(d) x_4[n] = \frac{\sin(0.25\pi n)}{9\pi n}$$

P-7.2 Determine the inverse DTFT of each of the following transforms:

$$(a) Y_1(e^{j\hat{\omega}}) = 2\pi$$

$$(b) Y_2(e^{j\hat{\omega}}) = 5e^{-j3\hat{\omega}}$$

$$(c) Y_3(e^{j\hat{\omega}}) = 6 \cos(3\hat{\omega})$$

$$(d) Y_4(e^{j\hat{\omega}}) = j \sin(7\hat{\omega})$$

P-7.3 Determine the inverse or forward DTFT as appropriate:

$$(a) V_1(e^{j\hat{\omega}}) = \begin{cases} 1 & |\hat{\omega}| \leq 0.3\pi \\ 0 & 0.3\pi < |\hat{\omega}| \leq \pi \end{cases}$$

$$(b) v_2[n] = \begin{cases} 0 & n < 0 \\ 1 & n = 0, 1, \dots, 9 \\ 0 & n > 9 \end{cases}$$

$$(c) V_3(e^{j\hat{\omega}}) = \begin{cases} 0 & |\hat{\omega}| \leq 0.3\pi \\ 1 & 0.3\pi < |\hat{\omega}| \leq \pi \end{cases}$$

$$(d) v_4[n] = \begin{cases} 0 & n < 0 \\ (-1)^n & n = 0, 1, \dots, 9 \\ 0 & n > 9 \end{cases}$$

P-7.4 Determine the DTFT of each of the following sequences:

$$(a) h_1[n] = 5\delta[n] - \frac{\sin(0.25\pi n)}{0.2\pi n}$$

$$(b) h_2[n] = \frac{\sin(0.4\pi n)}{0.1\pi n} - \frac{\sin(0.1\pi n)}{0.1\pi n}$$

$$(c) h_2[n] = \frac{\sin(0.4\pi(n-8))}{\pi(n-8)} - \frac{\sin(5\pi(n-8))}{\pi(n-8)}$$

P-7.5 Consider an LTI system defined by the difference equation

$$y[n] = 3x[n-2] + 3x[n-3] + 3x[n-4] + 3x[n-5] + 3x[n-6] = \sum_{k=2}^6 3x[n-k]$$

The frequency response of this system can be expressed in the following “Dirichlet-like” form:

$$H(e^{j\hat{\omega}}) = \alpha \left(\frac{\sin(L\hat{\omega}/2)}{\sin(\hat{\omega}/2)} \right) e^{-j\beta\hat{\omega}}$$

Determine the parameters L , α , and β .

P-7.6 The DTFT must be periodic with a period equal to 2π , so it is sufficient to define the DTFT for $-\pi \leq \hat{\omega} < \pi$. For each of the following ideal filters, determine the inverse transform of the given DTFT:

$$\begin{aligned} \text{(a)} \quad G_1(e^{j\hat{\omega}}) &= \begin{cases} 5e^{-j0.3\hat{\omega}} & 0 \leq |\hat{\omega}| \leq 0.4\pi \\ 0 & 0.4\pi < |\hat{\omega}| \leq \pi \end{cases} \\ \text{(b)} \quad G_2(e^{j\hat{\omega}}) &= \begin{cases} 0 & 0 \leq |\hat{\omega}| \leq 0.7\pi \\ 4e^{-j0.1\hat{\omega}} & 0.7\pi < |\hat{\omega}| \leq \pi \end{cases} \\ \text{(c)} \quad G_3(e^{j\hat{\omega}}) &= \begin{cases} 0 & 0 \leq |\hat{\omega}| \leq 0.4\pi \\ 9e^{-j0.2\hat{\omega}} & 0.4\pi < |\hat{\omega}| \leq 0.7\pi \\ 0 & 0.7\pi < |\hat{\omega}| \leq \pi \end{cases} \end{aligned}$$

P-7.7 The convolution property of the DTFT can simplify difficult operations that arise in LTI filtering. Simplify the following:

$$\begin{aligned} \text{(a)} \quad & \frac{\sin(0.25\pi n)}{9\pi n} * \frac{\sin(0.44\pi n)}{4\pi n} \\ \text{(b)} \quad & \frac{\sin(0.25\pi n)}{9\pi n} * \frac{\sin(0.25\pi n)}{8\pi n} * \frac{\sin(0.25\pi n)}{7\pi n} \\ \text{(c)} \quad & (0.3)^n u[n] * (-0.4)^{n-2} u[n-2] \quad (\text{requires partial fractions in the frequency domain}) \end{aligned}$$

P-7.8 The frequency response of an LTI system is $H(e^{j\hat{\omega}}) = \cos(3\hat{\omega})$. Determine the output of the system for each of the following input signals:

$$\begin{aligned} \text{(a)} \quad & x_1[n] = \delta[n-3] \\ \text{(b)} \quad & x_2[n] = 3 \cos(0.25\pi n) \\ \text{(c)} \quad & x_3[n] = u[n] - u[n-9] \end{aligned}$$

P-7.9 An example of the frequency-shifting property comes from modeling the response of a physical system as an oscillating signal whose amplitude is dropping. The precise form is an exponential times a sinusoid, $x[n] = a^n \cos(\hat{\omega}_0 n) u[n]$.

- (a) Use Euler's relation to show that we can express $x[n]$ as

$$x[n] = \frac{1}{2}e^{j\hat{\omega}_0 n} a^n u[n] + \frac{1}{2}e^{-j\hat{\omega}_0 n} a^n u[n]$$

- (b) By using the DTFT pair in (7.6), applying the frequency-shift property (7.25) twice, and finding a common denominator for the resulting two fractions, show that we can write $X(e^{j\hat{\omega}})$ as

$$X(e^{j\hat{\omega}}) = \frac{1 - a \cos(\hat{\omega}_0)e^{-j\hat{\omega}}}{(1 - ae^{j\hat{\omega}_0}e^{-j\hat{\omega}})(1 - ae^{-j\hat{\omega}_0}e^{-j\hat{\omega}})} = \frac{1 - a \cos(\hat{\omega}_0)e^{-j\hat{\omega}}}{1 - 2a \cos(\hat{\omega}_0)e^{-j\hat{\omega}} + a^2e^{-j\hat{\omega}2}}$$

P-7.10 For the signal $v[n] = a^n u[n]$, the DTFT $V(e^{j\hat{\omega}})$ can be found in Table 7-1. For the questions below, assume $a = 0.95$.

- (a) Make a plot of the magnitude $|V(e^{j\hat{\omega}})|$ for $-\pi < \hat{\omega} \leq \pi$.
- (b) If $V(e^{j\hat{\omega}})$ were a frequency response, is the filter lowpass, highpass, or bandpass?
- (c) Define $w[n] = v[n] \cos(0.3\pi n)$, and then make a plot of the magnitude $|W(e^{j\hat{\omega}})|$ for $-\pi < \hat{\omega} \leq \pi$.
- (d) If $W(e^{j\hat{\omega}})$ were a frequency response, is the filter lowpass, highpass, or bandpass?

P-7.11 Suppose that $H_{LP}(e^{j\hat{\omega}})$ is an ideal LPF with its bandedge at $\hat{\omega}_{co}$ as plotted in Fig. 7-5.

- (a) Show that the frequency response of an ideal HPF with cutoff frequency $\hat{\omega}_{co}$ can be represented by

$$H_{HP}(e^{j\hat{\omega}}) = 1 - H_{LP}(e^{j\hat{\omega}})$$

Hint: Try plotting the function $1 - H_{LP}(e^{j\hat{\omega}})$.

- (b) Use the result of part (a) to determine an expression for the impulse response $h_{HP}[n]$ of the HPF.

P-7.12 Suppose that $H_{BP}(e^{j\hat{\omega}})$ is an ideal BPF with its bandedges at $\hat{\omega}_{co1}$ and $\hat{\omega}_{co2}$ as in (7.51) and as plotted in Fig. 7-8.

- (a) Show that the frequency response of an ideal BPF with cutoff frequencies $\hat{\omega}_{co1} = 0.3\pi$ and $\hat{\omega}_{co2} = 0.6\pi$ can be represented as the difference of two ideal LPFs as in

$$H_{BP}(e^{j\hat{\omega}}) = H_{LP1}(e^{j\hat{\omega}}) - H_{LP2}(e^{j\hat{\omega}})$$

In particular, give the cutoff frequencies of the two LPFs, $H_{LP1}(e^{j\hat{\omega}})$ and $H_{LP2}(e^{j\hat{\omega}})$.

- (b) Use the result of part (a) to determine an expression for the impulse response $h_{\text{BP}}[n]$ of the BPF.

P-7.13 Consider the left-sided exponential sequence defined by

$$x[n] = -b^n u[-n - 1]$$

- (a) Sketch $x[n]$ for the case $b = 2$.
- (b) For what values of b does the DTFT of $x[n]$ exist?
- (c) Show that for the values of b found in part (b), the DTFT of $x[n]$ is

$$X(e^{j\hat{\omega}}) = \frac{1}{1 - be^{-j\hat{\omega}}}$$

P-7.14 Use Parseval's Theorem and the DTFT to evaluate:

(a)
$$\sum_{n=-\infty}^{\infty} \left| \frac{\sin(0.25\pi n)}{3\pi n} \right|^2$$

(b)
$$\sum_{n=1}^{\infty} \left| \frac{1}{\pi n} \right|^2$$

P-7.15 Use the DTFT to determine the autocorrelation function for each of the following signals:

- (a) $\delta[n - 4]$
- (b) $\delta[n - 4] - \delta[n - 6]$
- (c) $u[n - 6] - u[n - 16]$
- (d) $\frac{\sin(0.25\pi n)}{9\pi n}$

P-7.16 Consider the signal $x[n] = u[n] - u[n - 5]$

- (a) Determine $c_{xx}[n]$, the autocorrelation function (acf) of this signal.
- (b) Determine the DTFT of the acf; verify that it is purely real and nonnegative.
- (c) Determine the acf of the signal $y[n] = x[n - 2]$.

Hints: since the peak value of an acf must always be at zero lag, consider the possibility that $c_{yy}[n]$ might be the same as $c_{xx}[n]$. Working with the DTFT of the acf might be easier.

P-7.17 Use the `filterdesign` GUI (available on the web site) to create the impulse response of an FIR HPF with the following specifications: filter order $M = 32$, cutoff frequency $\hat{\omega}_{\text{co}} = 0.6\pi$, Hamming window.

- Make a plot of the frequency response magnitude; and also two “zoomed in” plots to show details of the passband and stopband magnitudes.
- From the plots in the previous part measure the passband and stopband edges, as well as the passband and stopband ripples (i.e., the parameters $\hat{\omega}_p$, $\hat{\omega}_s$, δ_p , and δ_s).
- If the filter order were changed to $M = 80$, estimate the change in the passband and stopband edges. Note: the ripples should not change much.
- Design the order-80 filter and measure the new passband and stopband edges. Comment on the accuracy of the estimate in the previous part.

P-7.18 Use the `filterdesign` GUI to create the impulse response of an FIR HPF with the Hamming window method. Use the following specifications: filter order $M = 32$, cutoff frequency $\hat{\omega}_{co} = 0.6\pi$. The questions below deal with filtering specific input signals and determining the corresponding output signals.

- When the input $x_1[n]$ is DC with a DC level of 10, determine the output level.
- When the input is the sinusoid $x_2[n] = 10 \cos(0.3\pi n)$ with zero phase, determine the output in the standard form $y_2[n] = A_2 \cos(\hat{\omega}n + \varphi_2)$.
- When the input is the sinusoid $x_3[n] = 10 \cos(0.8\pi n)$ with zero phase, determine the output in the standard form $y_3[n] = A_3 \cos(\hat{\omega}n + \varphi_3)$.

P-7.19 Use the `filterdesign` GUI to create the impulse response of an FIR HPF with the Hamming window method. Use the following specifications: filter order $M = 32$, cutoff frequency $\hat{\omega}_{co} = 0.6\pi$. The questions below deal with filtering specific input signals and determining the corresponding output signals.

- When the input $x_1[n]$ is DC with a DC level of 10, determine the output level $y_1[n]$.
- When the input is the sinusoid $x_2[n] = 10 \cos(0.3\pi n)$ with zero phase, determine the output in the standard form $y_2[n] = A_2 \cos(\hat{\omega}n + \varphi_2)$.
- Use MATLAB to verify the outputs in the previous parts. Generate 100 values of the signal $s[n] = x_1[n] + x_2[n] = 10 + 10 \cos(0.3\pi n)u[n]$ in a vector `sn` and filter the signal `sn` with MATLAB’s `filter` command to obtain `snOutput`. Plot `snOutput` for `n=0:99`. For comparison plot $y_1[n] + y_2[n]$ from parts (a) and (b) over the same range.

Note: since the MATLAB-filtered signal starts at $n = 0$, there is a *transient* interval at beginning of the output where the two plots differ, but after $N = 32$ the match should be perfect. Thus, it might be helpful to subtract the two signals being compared, and plot the difference in order to accentuate the transient region.

P-7.20 Use the `filterdesign` GUI to create the impulse response of an FIR HPF with the Hamming window method. Use the following specifications: filter order $M = 32$, cutoff frequency $\hat{\omega}_{co} = 0.6\pi$. The questions below deal with filtering specific input signals and determining the corresponding output signals.

- (a) Suppose the input sinusoid has unknown frequency and zero phase $x[n] = 9 \cos(\hat{\omega}n)$. Determine the lowest frequency $\hat{\omega}$ where the output has amplitude equal to 9 (i.e., $y[n] = 9 \cos(\hat{\omega}n + \varphi)$). For the chosen frequency, determine the phase φ , and demonstrate that converting phase to time shift gives the proper value.
- (b) Determine all possible frequencies where the output is $y[n] = 9 \cos(\hat{\omega}n + \varphi)$ when the input is $x[n] = 9 \cos(\hat{\omega}n)$.
- (c) Determine all possible frequencies where the output is zero when the input is $x[n] = 9 \cos(\hat{\omega}n)$.